References

[1] Lin J, Xing B and Jin D 2023 Optical Bioimaging and Therapy *Adv Opt Mater* 11

[2] Wolfbeis O S 2015 An overview of nanoparticles commonly used in fluorescent bioimaging *Chem Soc Rev* 44 4743–68

[3] Fatima A, Ahmad M W, Al Saidi A K A, Choudhury A, Chang Y and Lee G H 2021 Recent advances in gadolinium-based contrast agents for bioimaging applications *Nanomaterials* 11 1–23

[4] Chawda N, Mishra S, Basu M, Chander H, Podder R, Mahapatra S K and Banerjee I 2019 Synthesis of gadolinium oxide nanocuboids for in vitro bioimaging applications *Mater Res Express* 6

[5] Fei-Peng Z, Guo-Tao C, Shou-Ju W, Ying L, Yu-Xia T, Ying T, Jian-Dong W, Chun-Yan W, Xin W, Jing S, Zhao-Gang T and Guang-Ming L 2016 Dual-modality imaging probes with high magnetic relaxivity and near-infrared fluorescence based highly aminated mesoporous silica nanoparticles *J Nanomater* 2016

[6] Keereweer S, Van Driel P B A A, Snoeks T J A, Kerrebijn J D F, De Jong R J B, Vahrmeijer A L, Sterenborg H J C M and Löwik C W G M 2013 Optical image-guided cancer surgery: Challenges and limitations *Clinical Cancer Research* 19 3745–54

[7] Etrych T, Lucas H, Janoušková O, Chytil P, Mueller T and Mäder K 2016 Fluorescence optical imaging in anticancer drug delivery *Journal of Controlled Release* 226 168–81

[8] Huang X, Li Z, Yu Z, Deng X, Xin Y and Jesionowski T 2019 Recent Advances in the Synthesis, Properties, and Biological Applications of Platinum Nanoclusters *J Nanomater* 2019

[9] Augustine R, Hasan A, Primavera R, Wilson R J, Thakor A S and Kevadiya B D 2020 Cellular uptake and retention of nanoparticles: Insights on particle properties and interaction with cellular components *Mater Today Commun* 25

[10] Anishur Rahman A T M, Vasilev K and Majewski P 2011 Ultra small Gd2O3 nanoparticles: Absorption and emission properties *J Colloid Interface Sci* 354 592–6

[11] Li Y, Feng L, Yan W, Hussain I, Su L and Tan B 2019 PVP-templated highly luminescent copper nanoclusters for sensing trinitrophenol and living cell imaging *Nanoscale* 11 1286–94

[12] Verma V K, Sabbarwal S, Srivastava P and Kumar M 2023 In-depth insight of thermodynamic and kinetic barrier for computation of nucleation rate and interfacial energy of ultra-small Gd2O3 nanoclusters utilizing non-isothermal thermogravimetric models *Phys Scr* 98

[13] Srivastava P, Sabbarwal S, Verma V K and Kumar M 2023 A novel approach for determination of nucleation rates and interfacial energy of metallic magnesium

nanoclusters at high temperature using non-isothermal TGA models *Chem Eng Sci* 265 118223

[14] Bhakta R K, Maharrey S, Stavila V, Highley A, Alam T, Majzoub E and Allendorf M 2012 Thermodynamics and kinetics of NaAlH 4 nanocluster decomposition *Physical Chemistry Chemical Physics* 14 8160–9

[15] Wang C X and Yang G W 2005 Thermodynamics of metastable phase nucleation at the nanoscale *Materials Science and Engineering R: Reports* 49 157–202

[16] Klein D H, Smith M D and Driy J A 1967 Homogeneous nucleation of magnesium hydroxide *Talanta* 14 937–40

[17] Kathmann S M, Schenter G K, Garrett B C, Chen B and Siepmann J I 2009 Thermodynamics and kinetics of nanoclusters controlling gas-to-particle nucleation *Journal of Physical Chemistry C* 113 10354–70

[18] Li Q, Fernandez-Martinez A, Lee B, Waychunas G A and Jun Y S 2014 Interfacial energies for heterogeneous nucleation of calcium carbonate on mica and quartz *Environ Sci Technol* 48 5745–53

[19] Kalidindi S B and Jagirdar B R 2009 Highly monodisperse colloidal magnesium nanoparticles by room temperature digestive ripening *Inorg Chem* 48 4524–9

[20] Nafsin N, Aguiar J A, Aoki T, Thron A M, van Benthem K and Castro R H R 2017 Thermodynamics versus kinetics of grain growth control in nanocrystalline zirconia *Acta Mater* 136 224–34

[21] Polte J 2015 Fundamental growth principles of colloidal metal nanoparticles - a new perspective *CrystEngComm* 17 6809–30

[22] Joop H and Sefcik J 2020 *The Handbook of Continuous Crystallization* (The Royal Society of Chemistry)

[23] Dirksen J A and Ring T A 1991 Fundamentals of crystallization: Kinetic effects on particle size distributions and morphology *Chem Eng Sci* 46 2389–427

[24] Sahoo A K, Banerjee S, Ghosh S S and Chattopadhyay A 2014 Simultaneous RGB emitting Au nanoclusters in chitosan nanoparticles for anticancer gene theranostics *ACS Appl Mater Interfaces* 6 712–24

[25] Chen Z, Qian S, Chen X, Gao W and Lin Y 2012 Protein-templated gold nanoclusters as fluorescence probes for the detection of methotrexate *Analyst* 137 4356–61

[26] Soleilhac A, Bertorelle F and Antoine R 2018 Sizing protein-templated gold nanoclusters by time resolved fluorescence anisotropy decay measurements *Spectrochim Acta A Mol Biomol Spectrosc* 193 283–8

[27] Tan R X, Wang Q H, Xiao T X and Meng J 2020 Size Control of Monodisperse Au Nanoparticles: Controlling Role of Polyoxometalate [SiW9O34]10– *Russian Journal of Inorganic Chemistry* 65 1276–81

[28] Zhang X D, Wu D, Shen X, Liu P X, Fan F Y and Fan S J 2012 In vivo renal clearance, biodistribution, toxicity of gold nanoclusters *Biomaterials* 33 4628–38

[29] Liao W Y, Li H J, Chang M Y, Tang A C L, Hoffman A S and Hsieh P C H 2013 Comprehensive characterizations of nanoparticle biodistribution following systemic injection in mice *Nanoscale* 5 11079–86

[30] Kryza D, Taleb J, Janier M, Marmuse L, Miladi I, Bonazza P, Louis C, Perriat P, Roux S, Tillement O and Billotey C 2011 Biodistribution study of nanometric hybrid gadolinium oxide particles as a multimodal SPECT/MR/optical imaging and theragnostic agent *Bioconjug Chem* 22 1145–52

[31] Sahoo K, Khare D, Srikrishna S, Dubey A K and Kumar M 2020 Development of luminescent atacamite nanoclusters for bioimaging and photothermal applications *Nanotechnology* 31

[32] Landheer D, Wu X, Morais J, Baumvol I J R, Pezzi R P, Miotti L, Lennard W N and Kim J K 2001 Thermal stability and diffusion in gadolinium silicate gate dielectric films *Appl Phys Lett* 79 2618–20

[33] Ho S L, Yue H, Lee S, Tegafaw T, Ahmad M Y, Liu S, Saidi A K A Al, Zhao D, Liu Y, Nam S W, Chae K S, Chang Y and Lee G H 2022 Mono and Multiple Tumor-Targeting Ligand-Coated Ultrasmall Gadolinium Oxide Nanoparticles: Enhanced Tumor Imaging and Blood Circulation *Pharmaceutics* 14

[34] Garcia J, Liu S Z and Louie A Y 2017 Biological effects of MRI contrast agents: gadolinium retention, potential mechanisms and a role for phosphorus *Philosophical Transactions of the Royal Society A: Mathematical, Physical and Engineering Sciences* 375

[35] Srivastava P, Verma V K and Sabbarwal S soluble metallic magnesium nanoclusters for bioimaging applications

[36] Wang J Y, Chen J, Yang J, Wang H, Shen X, Sun Y M, Guo M and Zhang X D 2016 Effects of surface charges of gold nanoclusters on long-term in vivo biodistribution, toxicity, and cancer radiation therapy *Int J Nanomedicine* 11 3475–85

[37] Zhang X D, Wu D, Shen X, Liu P X, Fan F Y and Fan S J 2012 In vivo renal clearance, biodistribution, toxicity of gold nanoclusters *Biomaterials* 33 4628–38

[38] Sabbarwal S, Dubey A K, Pandey M and Kumar M 2020 Synthesis of biocompatible, BSA capped fluorescent CaCO3pre-nucleation nanoclusters for cell imaging applications *J Mater Chem B* 8 5729–44

[39] Jia D, Lu L and Yen W M 2002 Erbium energy levels relative to the band gap of gadolinium oxide *Opt Commun* 212 97–100

[40] Kumar Verma V, Srivastava P, Sabbarwal S, Singh M, Koch B and Kumar M 2022 White Light Emitting Gadolinium Oxide Nanoclusters for In-vitro Bio-imaging *ChemistrySelect* 7

[41] Shibu E S, Ono K, Sugino S, Nishioka A, Yasuda A, Shigeri Y, Wakida S I, Sawada M and Biju V 2013 Photouncaging nanoparticles for MRI and fluorescence imaging in vitro and in vivo *ACS Nano* 7 9851–9

[42] Zhang Y, Zhang B, Liu F, Luo J and Bai J 2013 In vivo tomographic imaging with fluorescence and MRI using tumor-targeted dual-labeled nanoparticles *Int J Nanomedicine* 9 33–41

[43] Evans T and Strezov L 2000 Interfacial heat transfer and nucleation of steel on metallic substrates *Metallurgical and Materials Transactions B: Process Metallurgy and Materials Processing Science* 31 1081–9

[44] Evans T and Strezov L 2000 Interfacial heat transfer and nucleation of steel on metallic substrates *Metallurgical and Materials Transactions B: Process Metallurgy and Materials Processing Science* 31 1081–9

[45] Li Q, Fernandez-Martinez A, Lee B, Waychunas G A and Jun Y S 2014 Interfacial energies for heterogeneous nucleation of calcium carbonate on mica and quartz *Environ Sci Technol* 48 5745–53

[46] Zhou Z Y, Tian N, Li J T, Broadwell I and Sun S G 2011 Nanomaterials of high surface energy with exceptional properties in catalysis and energy storage *Chem Soc Rev* 40 4167–85

[47] Online V A 2014 applications in cellular imaging and catalysis † 1775–81

[48] Bhandari U, Ayirizia B A, Malozovsky Y, Franklin L and Bagayoko D 2020 First principle investigation of electronic, transport, and bulk properties of zinc-blende magnesium sulfide *Electronics (Switzerland)* 9 1–9

[49] Mathur G, Nain S and Sharma P K 2015 Cancer: An Overview *Article in Academic Journal of Cancer Research* 8 1–09

[50] Gayathri T, Sundaram N M and Kumar R A 2015 Gadolinium oxide nanoparticles for Magnetic Resonance Imaging and cancer theranostics *Journal of Bionanoscience* 9 409–23

[51] Anon Home < https://www.wcrf.org/>-Cancer trends < https://www.wcrf.org/cancer-trends/>-Worldwide cancer data Worldwide cancer data

[52] Mole R H 1990 *Childhood cancer after prenatal exposure to diagnostic X-ray examinations in Britain* vol 62 (Macmillan Press Ltd)

[53] Yousaf T, Dervenoulas G and Politis M 2018 Advances in MRI Methodology *International Review of Neurobiology* vol 141 (Academic Press Inc.) pp 31–76

[54] Yang G, Song T, Wang M, Li M, Su Q, Xie Z, Xie X, Zhang H, Feng Y, Wu C, Liu Y and Yang H 2022 Recent Advancements in Nanosystem-Based Molecular Beacons for RNA Detection and Imaging *ACS Appl Nano Mater* 5 3065–86

[55] Warburtont N, Wood C, Lloyd C, Song S and Withers P 2003 *The 3-dimensional anatomy of the North-Western Marsupial Mole (Notoryctes caurinus Thomas 1920) using computed tomography, X-ray and magnetic resonance imaging* vol 22

[56] Söderlind F, Pedersen H, Petoral R M, Käll P O and Uvdal K 2005 Synthesis and characterization of Gd2O3 nanocrystals functionalized by organic acids *J Colloid Interface Sci* 288 140–8

[57] Tasman P 2017 synthesis and characterization of ultra-small gadolinium oxide nanoparticles a thesis submitted to the graduate school of natural and applied sciences of middle east technical university

[58] Gayathri T, Sundaram N M and Kumar R A 2015 Gadolinium oxide nanoparticles for Magnetic Resonance Imaging and cancer theranostics *Journal of Bionanoscience* 9 409–23

[59] Muhamad Sarih N, Myers P, Slater A, Slater B, Abdullah Z, Tajuddin H A and Maher S 2019 White Light Emission from a Simple Mixture of Fluorescent Organic Compounds *Sci Rep* 9 1–8

[60] Narayan S, Rajagopalan A, Reddy J S and Chadha A 2014 BSA binding to silica capped gold nanostructures: Effect of surface cap and conjugation design on nanostructure-BSA interface *RSC Adv* 4 1412–20

[61] Xiao X, Cai H, Huang Q, Wang B, Wang X, Luo Q, Li Y, Zhang H, Gong Q, Ma X, Gu Z and Luo K 2023 Polymeric dual-modal imaging nanoprobe with two-photon aggregation-induced emission for fluorescence imaging and gadolinium-chelation for magnetic resonance imaging *Bioact Mater* 19 538–49

[62] Sosnovik D E, Nahrendorf M, Deliolanis N, Novikov M, Aikawa E, Josephson L, Rosenzweig A, Weissleder R and Ntziachristos V 2007 Fluorescence tomography and magnetic resonance imaging of myocardial macrophage infiltration in infarcted myocardium in vivo *Circulation* 115 1384–91

[63] Zhao J, Chen J, Ma S, Liu Q, Huang L, Chen X, Lou K and Wang W 2018 Recent developments in multimodality fluorescence imaging probes *Acta Pharm Sin B* 8 320–38

[64] Kosaka N, Ogawa M, Choyke P L and Kobayashi H 2009 Clinical implications of near-infrared fluorescence imaging in cancer *Future Oncology* 5 1501–11

[65] Kalender W A 2006 X-ray computed tomography *Phys Med Biol* 51

[66] Vinegar H and Development Co S *X-Ray CT and NMR Imaging of Rocks*

[67] Hutchins G D, Miller M A, Soon V C and Receveur T *Small Animal PET Imaging*

[68] Ametamey S M, Honer M and Schubiger P A 2008 Molecular imaging with PET *Chem Rev* 108 1501–16

[69] Khalil M M, Tremoleda J L, Bayomy T B and Gsell W 2011 Molecular SPECT Imaging: An Overview *Int J Mol Imaging* 2011 1–15

[70] Schillaci O 2005 Hybrid SPECT/CT: A new era for SPECT imaging? *Eur J Nucl Med Mol Imaging* 32 521–4

[71] Deffieux T, Demené C and Tanter M 2021 Functional Ultrasound Imaging: A New Imaging Modality for Neuroscience *Neuroscience* 474 110–21

[72] Fenster A, Downey D B and Cardinal N 2001 *Three-dimensional ultrasound imaging INSTITUTE OF PHYSICS PUBLISHING PHYSICS IN MEDICINE Three-dimensional ultrasound imaging* vol 46

[73] Keereweer S, Kerrebijn J D F, Van Driel P B A A, Xie B, Kaijzel E L, Snoeks T J A, Que I, Hutteman M, Van Der Vorst J R, Mieog J S D, Vahrmeijer A L, Van De Velde C J H, Baatenburg De Jong R J and Löwik C W G M 2011 Optical image-guided surgery - Where do we stand? *Mol Imaging Biol* 13 199–207

[74] Lim J-W, Son S U and Lim E-K 2018 Recent Advances in Bioimaging for Cancer Research *State of the Art in Nano-bioimaging* (InTech)

[75] Cheng D, Liu R and Hu K 2022 Gold nanoclusters: Photophysical properties and photocatalytic applications *Front Chem* 10

[76] Yokoi T and Ishii K 2018 Dependence of phthalocyanine-based fluorescence on albumin structure: A fluorescent probe for ascorbic acid *J Photochem Photobiol A Chem* 364 1–5

[77] Ljubimova J Y, Fujita M, Ljubimov A V., Torchilin V P, Black K L and Holler E 2008 Poly(malic acid) nanoconjugates containing various antibodies and oligonucleotides for multitargeting drug delivery *Nanomedicine* 3 247–65

[78] Mondal P P and Diaspro A 2013 Point spread function engineering for super-resolution single-photon and multiphoton fluorescence microscopy *Advances in Imaging and Electron Physics* vol 175 (Academic Press Inc.) pp 201–19

[79] Cirtiu C M, Raychoudhury T, Ghoshal S and Moores A 2011 Systematic comparison of the size, surface characteristics and colloidal stability of zero valent iron nanoparticles pre- and post-grafted with common polymers *Colloids Surf A Physicochem Eng Asp* 390 95–104

[80] Soo Choi H, Liu W, Misra P, Tanaka E, Zimmer J P, Itty Ipe B, Bawendi M G and Frangioni J V. 2007 Renal clearance of quantum dots *Nat Biotechnol* 25 1165–70

[81] Lim E K, Kim T, Paik S, Haam S, Huh Y M and Lee K 2015 Nanomaterials for theranostics: Recent advances and future challenges *Chem Rev* 115 327–94

[82] Jiang S, Gnanasammandhan M K and Zhang Y 2009 Optical imaging-guided cancer therapy with fluorescent nanoparticles *J R Soc Interface* 7 3–18

[83] Phillips W T, Bao A, Brenner A J and Goins B A 2014 Image-guided interventional therapy for cancer with radiotherapeutic nanoparticles *Adv Drug Deliv Rev* 76 39–59

[84] Cheng Y, Morshed R A, Auffinger B, Tobias A L and Lesniak M S 2014 Multifunctional nanoparticles for brain tumor imaging and therapy *Adv Drug Deliv Rev* 66 42–57

[85] Tiwari D K, Tiwari M and Jin T 2020 Near-infrared fluorescent protein and bioluminescence-based probes for high-resolution in vivo optical imaging *Mater Adv* 1 967–87

[86] Shcherbakova D M, Baloban M, Emelyanov A V., Brenowitz M, Guo P and Verkhusha V V. 2016 Bright monomeric near-infrared fluorescent proteins as tags and biosensors for multiscale imaging *Nat Commun* 7

[87] Yan W, Zhang J, Abbas M, Li Y, Hussain S Z, Mumtaz S, Song Z, Hussain I and Tan B 2020 Facile synthesis of ultrastable fluorescent copper nanoclusters and their cellular imaging application *Nanomaterials* 10 1–12

[88] Wang X, Liu Z, Zhao W, Sun J, Qian B, Wang X, Zeng H, Du D and Duan J 2019 A novel switchable fluorescent sensor for facile and highly sensitive detection of alkaline phosphatase activity in a water environment with gold/silver nanoclusters *Anal Bioanal Chem* 411 1009–17

[89] Li W, Guo H, Li G, Chi Z, Chen H, Wang L, Liu Y, Chen K, Le M, Han Y, Yin L, Vajtai R, Ajayan P M, Weng Y and Wu M 2020 White luminescent single-crystalline chlorinated graphene quantum dots *Nanoscale Horiz* 5 928–33

[90] Lim J-W, Son S U and Lim E-K 2018 Recent Advances in Bioimaging for Cancer Research *State of the Art in Nano-bioimaging* (InTech)

[91] Kane R A 2004 *Intraoperative Ultrasonography History, Current State of the Art, and Future Directions*

[92] Bu L, Shen B and Cheng Z 2014 Fluorescent imaging of cancerous tissues for targeted surgery *Adv Drug Deliv Rev* 76 21–38

[93] De Veld D C G, Witjes M J H, Sterenborg H J C M and Roodenburg J L N 2005 The status of in vivo autofluorescence spectroscopy and imaging for oral oncology *Oral Oncol* 41 117–31

[94] Grubbe E H *PRIORITY IN THE THERAPEUTIC USE OF X-RAYS*

[95] Schaefer J, Sefcik M D, McKay R A, Dixon W T, Budinger T F and Lauterbur P C 1982 *38. A. Bax, Two-Dimensional Nuclear Magnetic Resonance in Liquids (Reidel* vol 86

[96] Smits M M, Tonneijck L, Muskiet M H A, Hoekstra T, Kramer M H H, Pieters I C, Cahen D L, Diamant M and Van Raalte D H Cardiovascular, renal and gastrointestinal effects of incretin-based therapies: an acute and 12-week randomised, double-blind, placebo-controlled, mechanistic intervention trial in type 2 diabetes

[97] Pautler R G, Silva A C and Koretsky A P 1998 *In Vivo Neuronal Tract Tracing Using Manganese-Enhanced Magnetic Resonance Imaging*

[98] Nekolla S G, Martinez-Moeller A and Saraste A 2009 PET and MRI in cardiac imaging: From validation studies to integrated applications *Eur J Nucl Med Mol Imaging* 36 121–30

[99] Sharp J C and King S B 2010 MRI using radiofrequency magnetic field phase gradients *Magn Reson Med* 63 151–61

[100] Barkhof F and Scheltens P 2002 *Imaging of White Matter Lesions* vol 13

[101] Soares D P and Law M 2009 Magnetic resonance spectroscopy of the brain: review of metabolites and clinical applications *Clin Radiol* 64 12–21

[102] Shahzad K and Mati W 2020 Advances in magnetic resonance imaging (MRI) *Advances in Medical and Surgical Engineering* (Elsevier) pp 121–42

[103] Arshiya Ara S, Katti G and Shireen A *Magnetic resonance imaging (MRI)-A review* vol 2011

[104] Song Y and Seo J K 2013 Conductivity and permittivity image reconstruction at the larmor frequency using MRI *SIAM J Appl Math* 73 2262–80

[105] Mugler J P 2014 Optimized three-dimensional fast-spin-echo MRI *Journal of Magnetic Resonance Imaging* 39 745–67

[106] Hanson L G 2008 Is quantum mechanics necessary for understanding magnetic resonance? *Concepts Magn Reson Part A Bridg Educ Res* 32 329–40

[107] Bloch F, Hansex W L and Packard A M *The Nuclear Induction Experiment*

[108] Zhang Y, Liu C, Deng H, Lin Y, Li J and Gao F 2022 Peridynamic Simulation of Heterogeneous Rock Based on Digital Image Processing and Low-Field Nuclear Magnetic Resonance Imaging *International Journal of Geomechanics* 22

[109] Louro R O 2013 Chapter 4 - Introduction to Biomolecular NMR and Metals *Practical Approaches to Biological Inorganic Chemistry* 77–107

[110] Rinck P A 2021 *Magnetic Resonance in Medicine Relaxation Times and Basic Pulse Sequences An Offprint from Magnetic Resonance in Medicine*

[111] Kingsley P B 1999 *Methods of Measuring ( ) Spin-Lattice T Relaxation 1 Times: An Annotated Bibliography* vol 11 (John Wiley & Sons)

[112] Lin C, Bernstein M, Huston J and Fain S 2001 *Measurements of T1 Relaxation times at 3.0T: Implications for clinical MRA* vol 9

[113] Pooley R A 2005 Fundamental physics of MR imaging *Radiographics* 25 1087–99

[114] Currie S, Hoggard N, Craven I J, Hadjivassiliou M and Wilkinson I D 2013 Understanding MRI: Basic MR physics for physicians *Postgrad Med J* 89 209–23

[115] Mantle M D, Sederman A J and Gladden L F *Single-and two-phase #ow in "xed-bed reactors: MRI #ow visualisation and lattice-Boltzmann simulations*

[116] Mekuria S L, Debele T A and Tsai H C 2017 Encapsulation of Gadolinium Oxide Nanoparticle (Gd2O3) Contrasting Agents in PAMAM Dendrimer Templates for Enhanced Magnetic Resonance Imaging in Vivo *ACS Appl Mater Interfaces* 9 6782–95

[117] Kaser B 1994 *COMPUTED TOMOGRAPHY AND MAGNETIC RESONANCE IMAGING OF THE NORMAL EQUINE CARPUS* vol 35

[118] Gaustad J V, Brurberg K G, Simonsen T G, Mollatt C S and Rofstad E K 2008 Tumor vascularity assessed by magnetic resonance imaging and intravital microscopy imaging *Neoplasia* 10 354–62

[119] Weinmann H J, Mühler A and Radüchel B 2007 Gadolinium Chelates: Chemistry, Safety, and Behavior *eMagRes* 2007

[120] Xiao Y D, Paudel R, Liu J, Ma C, Zhang Z S and Zhou S K 2016 MRI contrast agents: Classification and application (Review) *Int J Mol Med* 38 1319–26

[121] Serkova N J 2017 Nanoparticle-based magnetic resonance imaging on tumor-associated macrophages and inflammation *Front Immunol* 8

[122] Alipour A, Soran-Erdem Z, Utkur M, Sharma V K, Algin O, Saritas E U and Demir H V 2018 A new class of cubic SPIONs as a dual-mode T1 and T2 contrast agent for MRI *Magn Reson Imaging* 49 16–24

[123] Ma X, Gong A, Chen B, Zheng J, Chen T, Shen Z and Wu A 2015 Exploring a new SPION-based MRI contrast agent with excellent water-dispersibility, high specificity to cancer cells and strong MR imaging efficacy *Colloids Surf B Biointerfaces* 126 44–9

[124] Thangudu S, Huang E Y and Su C H 2022 Safe magnetic resonance imaging on biocompatible nanoformulations *Biomaterials Science* vol 10 (Royal Society of Chemistry) pp 5032–53

[125] Karthik V, Poornima S, Vigneshwaran A, Raj D P R D D, Subbaiya R, Manikandan S and Saravanan M 2021 Nanoarchitectonics is an emerging drug/gene delivery and targeting strategy -a critical review *J Mol Struct* 1243

[126] Rybka J D 2019 Radiosensitizing properties of magnetic hyperthermia mediated by superparamagnetic iron oxide nanoparticles (SPIONs) on human cutaneous melanoma cell lines *Reports of Practical Oncology and Radiotherapy* 24 152–7

[127] Soliman M, Daruge P, Dertkigil S S J, De Avila Fernandes E, Negrao J R, de Aguiar Vilela Mitraud S, Sakuma E T I, Fernandes A R C, Zhang N, Huo A, Li Y J, Zhou F, Rodrigues B M, Mohanta A, Blanchette V S and Doria A S 2017 Imaging of haemophilic arthropathy in growing joints: pitfalls in ultrasound and MRI *Haemophilia* 23 660–72

[128] Zhang B, Li Q, Yin P, Rui Y, Qiu Y, Wang Y and Shi D 2012 Ultrasound-triggered BSA/SPION hybrid nanoclusters for liver-specific magnetic resonance imaging *ACS Appl Mater Interfaces* 4 6479–86

[129] Ledwaba M, Masilela N, Nyokong T and Antunes E 2015 Surface modification of silica-coated gadolinium oxide nanoparticles with zinc tetracarboxyphenoxy phthalocyanine for the photodegradation of Orange G *J Mol Catal A Chem* 403 64–76

[130] Tran D H, Putri W B K, Wie C H, Kang B, Lee N H, Kang W N, Lee J Y and Seong W K 2012 Enhanced critical current density in GdBa2Cu3O 7 - δ thin films with substrate surface decoration using Gd2O3 nanoparticles *Thin Solid Films* 526 241–5

[131] Mishra S K and Kannan S 2017 Doxorubicin-Conjugated Bimetallic Silver-Gadolinium Nanoalloy for Multimodal MRI-CT-Optical Imaging and pH-Responsive Drug Release *ACS Biomater Sci Eng* 3 3607–19

[132] Xu C, Wang Y, Zhang C, Jia Y, Luo Y and Gao X 2017 AuGd integrated nanoprobes for optical/MRI/CT triple-modal in vivo tumor imaging *Nanoscale* 9 4620–8

[133] Das G K, Heng B C, Ng S C, White T, Loo J S C, D'Silva L, Padmanabhan P, Bhakoo K K, Selvan S T and Tan T T Y 2010 Gadolinium oxide ultranarrow nanorods as multimodal contrast agents for optical and magnetic resonance imaging *Langmuir* 26 8959–65

[134] Dai Y, Wu C, Wang S, Li Q, Zhang M, Li J and Xu K 2018 Comparative study on in vivo behavior of PEGylated gadolinium oxide nanoparticles and Magnevist as MRI contrast agent *Nanomedicine* 14 547–55

[135] Hifumi H, Yamaoka S, Tanimoto A, Citterio D and Suzuki K 2006 Gadolinium-based hybrid nanoparticles as a positive MR contrast agent *J Am Chem Soc* 128 15090–1

[136] Tweedle M F, Spielman Professor of Radiology S, Kanal E, Professor of Radiology F and Muller R 2014 *CONSIDERATIONS IN THE SELECTION OF A NEW GADOLINIUM-BASED CONTRAST AGENT THE JOURNAL OF PRACTICAL MEDICAL IMAGING AND MANAGEMENT SUPPLEMENT TO Considerations in the Selection of a New Gadolinium-Based Contrast Agent CE Credits Available*

[137] Anon Dotarem OMnni

[138] Ramalho J, Semelka R C, Ramalho M, Nunes R H, AlObaidy M and Castillo M 2016 Gadolinium-based contrast agent accumulation and toxicity: An update *American Journal of Neuroradiology* 37 1192–8

[139] Luo D, Cui S, Liu Y, Shi C, Song Q, Qin X, Zhang T, Xue Z and Wang T 2018 Biocompatibility of Magnetic Resonance Imaging Nanoprobes Improved by Transformable Gadolinium Oxide Nanocoils *J Am Chem Soc* 140 14211–6

[140] Radhika S P, Sreeram K J and Unni Nair B 2014 Mo-doped cerium gadolinium oxide as environmentally sustainable yellow pigments *ACS Sustain Chem Eng* 2 1251–6

[141] Esqueda A C, López J A, Andreu-de-Riquer G, Alvarado-Monzón J C, Ratnakar J, Lubag A J M, Sherry A D and De León-Rodríguez L M 2009 A new gadolinium-based MRI zinc sensor *J Am Chem Soc* 131 11387–91

[142] Her J L, Wu M H, Peng Y B, Pan T M, Weng W H, Pang S T and Chi L 2013 High performance GdTixOy electrolyte-insulator-semiconductor pH sensor and biosensor *Int J Electrochem Sci* 8 606–20

[143] Li Y, Li Y, Cai M, Li B, Huang F, Lei R and Xu S 2021 Enhanced tunable mid-infrared emissions by controlling rare earth ion energy transfer processes in multifunctional multiphase solids *J Eur Ceram Soc* 41 5981–9

[144] Park K and Olander D R 1992 *Defect models for the oxygen potentials of gadolinium-and europium-doped Urania* vol 187

[145] Mekuria S L, Debele T A and Tsai H C 2017 Encapsulation of Gadolinium Oxide Nanoparticle (Gd2O3) Contrasting Agents in PAMAM Dendrimer Templates for Enhanced Magnetic Resonance Imaging in Vivo *ACS Appl Mater Interfaces* 9 6782–95

[146] Jeyarani W J, Tenkyong T, Bachan N, Kumar D A and Shyla J M 2016 An investigation on the tuning effect of glucose-capping on the size and bandgap of CuO nanoparticles *Advanced Powder Technology* 27 338–46

[147] Rowe M D, Tham D H, Kraft S L and Boyes S G 2009 Polymer-modified gadolinium metal-organic framework nanoparticles used as multifunctional nanomedicines for the targeted imaging and treatment of cancer *Biomacromolecules* vol 10 pp 983–93

[148] Aashima, Pandey S K, Singh S and Mehta S K 2018 Ultrasonication assisted fabrication of L-lysine functionalized gadolinium oxide nanoparticles and its biological acceptability *Ultrason Sonochem* 49 53–62

[149] Harstad S, Hunagund S, Boekelheide Z, Hussein Z A, El-Gendy A A and Hadimani R L 2018 Gd-Based Magnetic Nanoparticles for Biomedical Applications *Magnetic Nanostructured Materials: From Lab to Fab* (Elsevier) pp 137–55

[150] Mignot A, Truillet C, Lux F, Sancey L, Louis C, Denat F, Boschetti F, Bocher L, Gloter A, Stéphan O, Antoine R, Dugourd P, Luneau D, Novitchi G, Figueiredo L C, De Morais P C, Bonneviot L, Albela B, Ribot F, Van Lokeren L, Déchamps-Olivier I, Chuburu F, Lemercier G, Villiers C, Marche P N, Le Duc G, Roux S, Tillement O and Perriat P 2013 A top-down synthesis route to ultrasmall multifunctional Gd-based silica nanoparticles for theranostic applications *Chemistry - A European Journal* 19 6122–36

[151] Gan Y X, Jayatissa A H, Yu Z, Chen X and Li M 2020 Hydrothermal Synthesis of Nanomaterials *J Nanomater* 2020

[152] Vahdatkhah P, Madaah Hosseini H R, Khodaei A, Montazerabadi A R, Irajirad R, Oghabian M A and Delavari H. H 2015 Rapid microwave-assisted synthesis of PVP-coated ultrasmall gadolinium oxide nanoparticles for magnetic resonance imaging *Chem Phys* 453–454 35–41

[153] Khakpour Z, Youzbashi A A, Maghsoudipour A and Ahmadi K 2011 Synthesis of nanosized gadolinium doped ceria solid solution by high energy ball milling *Powder Technol* 214 117–21

[154] Chen F, Chen M, Yang C, Liu J, Luo N, Yang G, Chen D and Li L 2015 Terbium-doped gadolinium oxide nanoparticles prepared by laser ablation in liquid for use as a fluorescence and magnetic resonance imaging dual-modal contrast agent *Physical Chemistry Chemical Physics* 17 1189–96

[155] Marwani H M, Ahmad S and Rahman M M 2022 Catalytic Reduction of Environmental Pollutants with Biopolymer Hydrogel Cross-Linked Gelatin Conjugated Tin-Doped Gadolinium Oxide Nanocomposites *Gels* 8

[156] Chaudhary S, Kumar S, Kumar S, Chaudhary G R, Mehta S K and Umar A 2019 Ethylene glycol functionalized gadolinium oxide nanoparticles as a potential electrochemical sensing platform for hydrazine and p-nitrophenol *Coatings* 9

[157] Rajan A R and Philip D 2019 Catalytic and cytotoxic activity of PEG capped gadolinium oxide nanoparticles *AIP Conference Proceedings* vol 2082 (American Institute of Physics Inc.)

[158] Lalwani G, Sundararaj J L, Schaefer K, Button T and Sitharaman B 2014 Synthesis, characterization, in vitro phantom imaging, and cytotoxicity of a novel graphene-based multimodal magnetic resonance imaging-X-ray computed tomography contrast agent *J Mater Chem B* 2 3519–30

[159] Manikam V R, Cheong K Y and Razak K A 2011 Chemical reduction methods for synthesizing Ag and Al nanoparticles and their respective nanoalloys *Mater Sci Eng B Solid State Mater Adv Technol* 176 187–203

[160] Yan Y, Zhao J, Luo J and Lee J M 2017 Hierarchical Gadolinium Oxide Microspheres for Enzymeless Electro-biosensors in Hydrogen Peroxide Dynamic Detection *ChemElectroChem* 4 272–7

[161] Hazarika S, Paul N and Mohanta D 2014 *Rapid hydrothermal route to synthesize cubic-phase gadolinium oxide nanorods* vol 37

[162] Chuang K T and Lin Y W 2017 Microwave-Assisted Formation of Gold Nanoclusters Capped in Bovine Serum Albumin and Exhibiting Red or Blue Emission *Journal of Physical Chemistry C* 121 26997–7003

[163] Kaur N, Singh A and Ahmad W 2023 Microwave Assisted Green Synthesis of Silver Nanoparticles and Its Application: A Review *J Inorg Organomet Polym Mater* 33 663–72

[164] Fendler J H 1997 Biomineralization inspired preparation of nanoparticles and nanoparticulate films *Current Opinion in Solid St&e & Msterisls Sdence* 2 365–9

[165] Mann S 1995 *Biomineralization and Biomimetic Materials Chemistry* vol 5

[166] Ghavam M, Dastan D, Fadaei E and Chehardoli G 2021 Synthesis of Gadolinium Complexes Using Medicinal Plant Extracts *Avicenna Journal of Pharmaceutical Research* 2 44–8

[167] Khan S A, Gambhir S and Ahmad A 2014 Extracellular biosynthesis of gadolinium oxide (Gd2O3) nanoparticles, their biodistribution and bioconjugation with the chemically modified anticancer drug taxol *Beilstein Journal of Nanotechnology* 5 249–57

[168] Rajan A R, Rajan A, John A, Vilas V and Philip D 2019 Biogenic synthesis of nanostructured Gd2O3: Structural, optical and bioactive properties *Ceram Int* 45 21947–52

[169] Zhao J, Zhang Q, Liu W, Shan G and Wang X 2021 Biocompatible BSA-Ag2S Nanoparticles for Photothermal Therapy of Cancer *Colloids Surf B Biointerfaces* 211 112295

[170] Lillo C R, Calienni M N, Rivas Aiello B, Prieto M J, Rodriguez Sartori D, Tuninetti J, Toledo P, Alonso S del V, Moya S, Gonzalez M C, Montanari J and Soler-Illia G J A A 2020 BSA-capped gold nanoclusters as potential theragnostic for skin diseases: Photoactivation, skin penetration, in vitro, and in vivo toxicity *Materials Science and Engineering C* 112 110891

[171] Yadav P and Yadav A B 2021 Preparation and characterization of BSA as a model protein loaded chitosan nanoparticles for the development of protein-/peptide-based drug delivery system *Futur J Pharm Sci* 7

[172] Zhou C, Wu H, Huang C, Wang M and Jia N 2014 Facile synthesis of single-phase mesoporous Gd2O3:Eu Nanorods and their application for drug delivery and multimodal imaging *Particle and Particle Systems Characterization* 31 675–84

[173] Siddiqi K S, Husen A and Rao R A K 2018 A review on biosynthesis of silver nanoparticles and their biocidal properties *J Nanobiotechnology* 16

[174] Cui H, Zayat M and Levy D 2005 *Sol-Gel Synthesis of Nanoscaled Spinels Using Propylene Oxide as a Gelation Agent* vol 35

[175] Niederberger M 2007 Nonaqueous sol-gel routes to metal oxide nanoparticles *AccChem Res* 40 793–800

[176] Parashar M, Shukla V K and Singh R 2020 Metal oxides nanoparticles via sol–gel method: a review on synthesis, characterization and applications *Journal of Materials Science: Materials in Electronics* 31 3729–49

[177] Hasnidawani J N, Azlina H N, Norita H, Bonnia N N, Ratim S and Ali E S 2016 Synthesis of ZnO Nanostructures Using Sol-Gel Method *Procedia Chem* 19 211–6

[178] Rahman I A, Vejayakumaran P, Sipaut C S, Ismail J and Chee C K 2008 Effect of the drying techniques on the morphology of silica nanoparticles synthesized via sol-gel process *Ceram Int* 34 2059–66

[179] Anishur Rahman A T M, Majewski P and Vasilev K 2013 Gd 2O 3 nanoparticles: Size-dependent nuclear magnetic resonance *Contrast Media Mol Imaging* 8 92–5

[180] Faucher L, Tremblay M, Lagueux J, Gossuin Y and Fortin M A 2012 Rapid synthesis of PEGylated ultrasmall gadolinium oxide nanoparticles for cell labeling and tracking with MRI *ACS Appl Mater Interfaces* 4 4506–15

[181] Khan S, Shah Z H, Riaz S, Ahmad N, Islam S, Raza M A and Naseem S 2020 Antimicrobial activity of citric acid functionalized iron oxide nanoparticles – Superparamagnetic effect *Ceram Int* 46 10942–51

[182] Otsuka H, Nagasaki Y and Kataoka K 2004 Characterization of aldehyde-PEG tethered surfaces: Influence of PEG chain length on the specific biorecognition *Langmuir* 20 11285–7

[183] Gidi Y, Bayram S, Ablenas C J, Blum A S and Cosa G 2018 Efficient One-Step PEG-Silane Passivation of Glass Surfaces for Single-Molecule Fluorescence Studies *ACS Appl Mater Interfaces* 10 39505–11

[184] Koczkur K M, Mourdikoudis S, Polavarapu L and Skrabalak S E 2015 Polyvinylpyrrolidone (PVP) in nanoparticle synthesis *Dalton Transactions* 44 17883–905

[185] Arsalani N, Fattahi H and Nazarpoor M 2010 Synthesis and characterization of PVP-functionalized superparamagnetic Fe 3O 4 nanoparticles as an MRI contrast agent *Express Polym Lett* 4 329–38

[186] Sadeghi B, Sadjadi M A S and Pourahmad A *Effects of protective agents (PVA & PVP) on the formation of silver nanoparticles* vol 3

[187] Siribbal S M, Ilyas S, Renner A M, Iqbal S, Muñoz Vázquez S, Moawia A, Valldor M, Hussain M S, Schomäcker K and Mathur S 2022 Click functionalized biocompatible gadolinium oxide core-shell nanocarriers for imaging of breast cancer cells *RSC Adv* 12 31830–45

[188] Chen Y C, Huang X C, Luo Y L, Chang Y C, Hsieh Y Z and Hsu H Y 2013 Non-metallic nanomaterials in cancer theranostics: A review of silica- and carbon-based drug delivery systems *Sci Technol Adv Mater* 14

[189] Bennett K M, Jo J I, Cabral H, Bakalova R and Aoki I 2014 MR imaging techniques for nano-pathophysiology and theranostics *Adv Drug Deliv Rev* 74 75–94

[190] Cardoso M M, Peça I N and Roque A C A 2012 *Antibody-Conjugated Nanoparticles for Therapeutic Applications* vol 19

[191] Incram G A *Substances involved in the natural resistance of fish to infection-A review* vol 16

[192] Arruebo M, Valladares M and González-Fernández Á 2009 Antibody-conjugated nanoparticles for biomedical applications *J Nanomater* 2009

[193] Wang G, Peng Q and Li Y 2011 Lanthanide-doped nanocrystals: Synthesis, optical-magnetic properties, and applications *Acc Chem Res* 44 322–32

[194] Zhou L, Gu Z, Liu X, Yin W, Tian G, Yan L, Jin S, Ren W, Xing G, Li W, Chang X, Hu Z and Zhao Y 2012 Size-tunable synthesis of lanthanide-doped Gd 2O 3 nanoparticles and their applications for optical and magnetic resonance imaging *J Mater Chem* 22 966–74

[195] Jaishankar M, Tseten T, Anbalagan N, Mathew B B and Beeregowda K N 2014 Toxicity, mechanism and health effects of some heavy metals *Interdiscip Toxicol* 7 60–72

[196] Fortin M A, Petoral R M, Söoderlind F, Klasson A, Engströöm M, Veres T, Käll P O and Uvdal K 2007 Polyethylene glycol-covered ultra-small Gd2O3 nanoparticles for positive contrast at 1.5 T magnetic resonance clinical scanning *Nanotechnology* 18

[197] Ahrén M, Selegård L, Söderlind F, Linares M, Kauczor J, Norman P, Käll P O and Uvdal K 2012 A simple polyol-free synthesis route to Gd2O3 nanoparticles for MRI applications: An experimental and theoretical study *Journal of Nanoparticle Research* 14

[198] Luo M, Xu L, Xia J, Zhao H, Du Y and Lei B 2020 Synthesis of porous gadolinium oxide nanosheets for cancer therapy and magnetic resonance imaging *Mater Lett* 265 127375

[199] Wahsner J, Gale E M, Rodríguez-Rodríguez A and Caravan P 2019 Chemistry of MRI contrast agents: Current challenges and new frontiers *Chem Rev* 119 957–1057

[200] Ramalho J, Semelka R C, Ramalho M, Nunes R H, AlObaidy M and Castillo M 2016 Gadolinium-based contrast agent accumulation and toxicity: An update *American Journal of Neuroradiology* 37 1192–8

[201] Vahdatkhah P, Madaah Hosseini H R, Khodaei A, Montazerabadi A R, Irajirad R, Oghabian M A and Delavari H. H 2015 Rapid microwave-assisted synthesis of PVP-coated ultrasmall gadolinium oxide nanoparticles for magnetic resonance imaging *Chem Phys* 453–454 35–41

[202] Anishur Rahman A T M, Vasilev K and Majewski P 2011 Ultra small Gd2O3 nanoparticles: Absorption and emission properties *J Colloid Interface Sci* 354 592–6

[203] Zhou L, Gu Z, Liu X, Yin W, Tian G, Yan L, Jin S, Ren W, Xing G, Li W, Chang X, Hu Z and Zhao Y 2012 Size-tunable synthesis of lanthanide-doped Gd 2O 3 nanoparticles and their applications for optical and magnetic resonance imaging *J Mater Chem* 22 966–74

[204] Ortega-Berlanga B, Betancourt-Mendiola L, Del Angel-Olarte C, Hernández-Adame L, Rosales-Mendoza S and Palestino G 2021 An overview of gadolinium-based oxide and oxysulfide particles: Synthesis, properties, and biomedical applications *Crystals (Basel)* 11 1–34

[205] Bridot J L, Faure A C, Laurent S, Rivière C, Billotey C, Hiba B, Janier M, Josserand V, Coll J L, Elst L Vander, Muller R, Roux S, Perriat P and Tillement O

2007 Hybrid gadolinium oxide nanoparticles: Multimodal contrast agents for in vivo imaging *J Am Chem Soc* 129 5076–84

[206] Ahrén M, Selegård L, Klasson A, Söderlind F, Abrikossova N, Skoglund C, Bengtsson T, Engström M, Käll P O and Uvdal K 2010 Synthesis and characterization of PEGylated Gd2O3 nanoparticles for MRI contrast enhancement *Langmuir* 26 5753–62

[207] Zhang W, Martinelli J, Mayer F, Bonnet C S, Szeremeta F and Djanashvili K 2015 Molecular architecture control in synthesis of spherical Ln-containing nanoparticles *RSC Adv* 5 69861–9

[208] Baig N, Kammakakam I, Falath W and Kammakakam I 2021 Nanomaterials: A review of synthesis methods, properties, recent progress, and challenges *Mater Adv* 2 1821–71

[209] Luo N, Tian X, Yang C, Xiao J, Hu W, Chen D and Li L 2013 Ligand-free gadolinium oxide for in vivo T1-weighted magnetic resonance imaging *Physical Chemistry Chemical Physics* 15 12235–40

[210] Faucher L, Tremblay M, Lagueux J, Gossuin Y and Fortin M A 2012 Rapid synthesis of PEGylated ultrasmall gadolinium oxide nanoparticles for cell labeling and tracking with MRI *ACS Appl Mater Interfaces* 4 4506–15

[211] Relaxivity L, Particle O, Park J Y, Baek M J, Choi E S, Woo S, Kim J H, Kim T J, Jung J C, Chae S, Chang Y and Lee G H 2009 Oxide Nanoparticles as Advanced T 1 *ACS Nano* 3 3663–9

[212] Han L, Xia J M, Hai X, Shu Y, Chen X W and Wang J H 2017 Protein-Stabilized Gadolinium Oxide-Gold Nanoclusters Hybrid for Multimodal Imaging and Drug Delivery *ACS Appl Mater Interfaces* 9 6941–9

[213] Trinh L H, Hoa T T, Van Hieu N and Cuong N D 2017 Facile Synthesis of Ultrafine Gd2O3 Nanoparticles by Polyol Microwave Method *J Electron Mater* 46 3484–90

[214] Thaninki L V, Arputharaj S N and Manasai A 2022 Facile wet chemical synthesis and characterization of zinc doped gadolinium oxide nanoparticles for enhanced photodegradation of Rhodamine B dye under illumination of UV light *Iranian Journal of Catalysis* 12 315–36

[215] Vahdatkhah P, Madaah Hosseini H R, Khodaei A, Montazerabadi A R, Irajirad R, Oghabian M A and Delavari H. H 2015 Rapid microwave-assisted synthesis of PVP-coated ultrasmall gadolinium oxide nanoparticles for magnetic resonance imaging *Chem Phys* 453–454 35–41

[216] Niftaliev S I, Kuznetsova I V., Saranov I A, Zhundrikova T V., Lygina L V., Tuneekov V Y, Chislova I V. and Zvereva I A 2019 Synthesis of Nanosized Gadolinium Oxide *Glass Physics and Chemistry* 45 232–7

[217] Chaudhary S, Kumar S and Mehta S K 2015 Glycol modified gadolinium oxide nanoparticles as a potential template for selective and sensitive detection of 4-nitrophenol *J Mater Chem C Mater* 3 8824–33

[218] Wu C, Cai R, Zhao T, Wu L, Zhang L, Jin J, Xu L, Li P, Li T, Zhang M and Du F 2020 Hyaluronic Acid-Functionalized Gadolinium Oxide Nanoparticles for Magnetic Resonance Imaging-Guided Radiotherapy of Tumors *Nanoscale Res Lett* 15

[219] Anon Part Part Syst Charact - 2014 - Zhou - Facile Synthesis of Single-Phase Mesoporous Gd2O3 Eu Nanorods and Their.pdf

[220] Surendra T V, Mohana Roopan S and Khan M R 2019 Biogenic approach to synthesize rod shaped Gd2O3 nanoparticles and its optimization using response surface methodology-Box–Behnken design model *Biotechnol Prog* 35 1–12

[221] Zhao X, Wang W, Zhang Y, Wu S, Li F and Liu J P 2014 Synthesis and characterization of gadolinium doped cobalt ferrite nanoparticles with enhanced adsorption capability for Congo Red *Chemical Engineering Journal* 250 164–74

[222] Chawda N R, Mahapatra S K and Banerjee I 2021 Surface-engineered gadolinium oxide nanorods and nanocuboids for bioimaging *Rare Metals* 40 848–57

[223] Shabanzadeh-Kouyakhi A 2022 Embedding Gd2O3 nanoparticles hydrothermally prepared in a Fe3O4 shell and surface modification with a dextrose bio capping agent *Ceram Int* 48 31326–33

[224] Aashima, Pandey S K, Singh S and Mehta S K 2018 Biocompatible gadolinium oxide nanoparticles as efficient agent against pathogenic bacteria *J Colloid Interface Sci* 529 496–504

[225] Han L, Xia J M, Hai X, Shu Y, Chen X W and Wang J H 2017 Protein-Stabilized Gadolinium Oxide-Gold Nanoclusters Hybrid for Multimodal Imaging and Drug Delivery *ACS Appl Mater Interfaces* 9 6941–9

[226] Lubis W Z, Azizah M and Caesariyanti R P 2022 The Effect of Conventional and Sonochemical Synthesis Methods on Gd2O3 Nanoparticles Properties 24 2614–087

[227] Sakai N, Zhu L, Kurokawa A, Takeuchi H, Yano S, Yanoh T, Wada N, Taira S, Hosokai Y, Usui A, Machida Y, Saito H and Ichiyanagi Y 2012 Synthesis of Gd2O3 nanoparticles for MRI contrast agents *J Phys Conf Ser* 352

[228] Shen Z, Fan W, Yang Z, Liu Y, Bregadze V I, Mandal S K, Yung B C, Lin L, Liu T, Tang W, Shan L, Liu Y, Zhu S, Wang S, Yang W, Bryant L H, Nguyen D T, Wu A and Chen X 2019 Exceedingly Small Gadolinium Oxide Nanoparticles with Remarkable Relaxivities for Magnetic Resonance Imaging of Tumors *Small* 15 1–9

[229] Xu W, Park J Y, Kattel K, Ahmad M W, Bony B A, Heo W C, Jin S, Park J W, Chang Y, Kim T J, Park J A, Do J Y, Chae K S and Lee G H 2012 Fluorescein-polyethyleneimine coated gadolinium oxide nanoparticles as T1 magnetic resonance imaging (MRI)-cell labeling (CL) dual agents *RSC Adv* 2 10907–15

[230] Hifumi H, Yamaoka S, Tanimoto A, Citterio D and Suzuki K 2006 Gadolinium-based hybrid nanoparticles as a positive MR contrast agent *J Am Chem Soc* 128 15090–1

[231] Kryza D, Taleb J, Janier M, Marmuse L, Miladi I, Bonazza P, Louis C, Perriat P, Roux S, Tillement O and Billotey C 2011 Biodistribution study of nanometric hybrid gadolinium oxide particles as a multimodal SPECT/MR/optical imaging and theragnostic agent *Bioconjug Chem* 22 1145–52

[232] Jamil M Z A M, Mohamed F, Rosli N R A M, Rahman I A, Idris M I, Bradley D A, Nor M M and Mustafa S N M 2019 Effect of gamma irradiation on magnetic gadolinium oxide nanoparticles coated with chitosan (GdNPs-Cs) as contrast agent in magnetic resonance imaging *Radiation Physics and Chemistry* 165 3–8

[233] Dědková K, Kuzníková, Pavelek L, Matějová K, Kupková J, Čech Barabaszová K, Váňa R, Burda J, Vlček J, Cvejn D and Kukutschová J 2017 Daylight induced antibacterial activity of gadolinium oxide, samarium oxide and erbium oxide nanoparticles and their aquatic toxicity *Mater Chem Phys* 197 226–35

[234] Chaturvedi A, Pranjali P, Meher M K, Raj R, Basak M, Singh R K, Poluri K M, Kumar D and Guleria A 2020 In vitro and ex vivo relaxometric properties of ethylene glycol coated gadolinium oxide nanoparticles for potential use as contrast agents in magnetic resonance imaging *J Appl Phys* 128

[235] Pranjali P, Tripathi D K, Chaturvedi A, Singh R K, Poluri K M, Kumar D and Guleria A 2023 Role of surface hydrophilicity on MR relaxivity of PEG coated-gadolinium oxide nanoparticles *Phys Scr* 98

[236] Zou Q, Passini L, Gibot L, Lagarde D, Hu J, Zhu H, Desmoulin F, Sicard P and Paiyabhroma N 2023 MATERIALS CHEMISTRY PVP-coated ultrasmall Nd-doped Gd 2 O 2 S nanoparticles for multimodal imaging †

[237] Alizadeh M J, Kariminezhad H, Monfared A S, Mostafazadeh A, Amani H, Niksirat F and Pourbagher R 2019 An experimental study about the application of Gadolinium oxide nanoparticles in magnetic theranostics *Mater Res Express* 6

[238] Osseni S A, Lechevallier S, Verelst M, Dujardin C, Dexpert-Ghys J, Neumeyer D, Leclercq M, Baaziz H, Cussac D, Santran V and Mauricot R 2011 New nanoplatform based on Gd2O2S: Eu3+ core: Synthesis, characterization and use for in vitro bio-labelling *J Mater Chem* 21 18365–72

[239] Liu Z, Liu X, Yuan Q, Dong K, Jiang L, Li Z, Ren J and Qu X 2012 Hybrid mesoporous gadolinium oxide nanorods: A platform for multimodal imaging and enhanced insoluble anticancer drug delivery with low systemic toxicity *J Mater Chem* 22 14982–90

[240] Singh G, McDonagh B H, Hak S, Peddis D, Bandopadhyay S, Sandvig I, Sandvig A and Glomm W R 2017 Synthesis of gadolinium oxide nanodisks and gadolinium doped iron oxide nanoparticles for MR contrast agents *J Mater Chem B* 5 418–22

[241] Zhang W, Martinelli J, Mayer F, Bonnet C S, Szeremeta F and Djanashvili K 2015 Molecular architecture control in synthesis of spherical Ln-containing nanoparticles *RSC Adv* 5 69861–9

[242] Vahdatkhah P, Madaah Hosseini H R, Khodaei A, Montazerabadi A R, Irajirad R, Oghabian M A and Delavari H. H 2015 Rapid microwave-assisted synthesis of

PVP-coated ultrasmall gadolinium oxide nanoparticles for magnetic resonance imaging *Chem Phys* 453–454 35–41

[243] Surendra T V, Mohana Roopan S and Khan M R 2019 Biogenic approach to synthesize rod shaped Gd2O3 nanoparticles and its optimization using response surface methodology-Box–Behnken design model *Biotechnol Prog* 35 1–12

[244] Akhtar M J, Ahamed M, Alhadlaq H and Alrokayan S 2019 Toxicity Mechanism of Gadolinium Oxide Nanoparticles and Gadolinium Ions in Human Breast Cancer Cells *Curr Drug Metab* 20 907–17

[245] Thangappan R, Kalaiselvam S, Elayaperumal A and Jayavel R 2012 Fabrication of Gd 2 O 3 nanofibers by electrospinning technique using PVA as a structure directing template *Appl Surf Sci* 261 770–3

[246] Wei Y, Zhong L, Li D, Ma Q and Dong X 2019 A novel strategy of fabricating GdOF:Er3+ nanofibers possessing upconversion luminescence and paramagnetic properties: The combination of electrospinning with fluoro-oxidation technique *Opt Mater (Amst)* 95

[247] Xu W, Park J Y, Kattel K, Ahmad M W, Bony B A, Heo W C, Jin S, Park J W, Chang Y, Kim T J, Park J A, Do J Y, Chae K S and Lee G H 2012 Fluorescein-polyethyleneimine coated gadolinium oxide nanoparticles as T1 magnetic resonance imaging (MRI)-cell labeling (CL) dual agents *RSC Adv* 2 10907–15

[248] Srivastava P, Sabbarwal S, Verma V K and Kumar M 2023 A novel approach for determination of nucleation rates and interfacial energy of metallic magnesium nanoclusters at high temperature using non-isothermal TGA models *Chem Eng Sci* 265 118223

[249] Bian J, Guo D, Li Y, Cai W, Hua Y and Cao X 2022 Homogeneous nucleation and condensation mechanism of methane gas: A molecular simulation perspective *Energy* 249 123610

[250] Singh S, Prasad Chakraborty J and Kumar Mondal M 2020 Intrinsic kinetics, thermodynamic parameters and reaction mechanism of non-isothermal degradation of torrefied Acacia nilotica using isoconversional methods *Fuel* 259 116263

[251] Fernandez-Martinez A, Hu Y, Lee B, Jun Y S and Waychunas G A 2013 In situ determination of interfacial energies between heterogeneously nucleated CaCO3 and quartz substrates: Thermodynamics of CO 2 mineral trapping *Environ Sci Technol* 47 102–9

[252] Evans T and Strezov L 2000 Interfacial heat transfer and nucleation of steel on metallic substrates *Metallurgical and Materials Transactions B: Process Metallurgy and Materials Processing Science* 31 1081–9

[253] Chaudhary S, Kumar S and Mehta S K 2015 Glycol modified gadolinium oxide nanoparticles as a potential template for selective and sensitive detection of 4-nitrophenol *J Mater Chem C Mater* 3 8824–33

[254] Kumar M, Sabbarwal S, Mishra P K and Upadhyay S N 2019 Thermal degradation kinetics of sugarcane leaves (Saccharum officinarum L) using thermo-gravimetric and differential scanning calorimetric studies *Bioresour Technol* 279 262–70

[255] Bhardwaj G, Kumar M, Mishra P K and Upadhyay S N 2023 Kinetic analysis of the slow pyrolysis of paper wastes *Biomass Convers Biorefin* 13 3087–100

[256] Wanjun T, Cunxin W and Donghua C 2006 An investigation of the pyrolysis kinetics of some aliphatic amino acids *J Anal Appl Pyrolysis* 75 49–53

[257] Starink M J 2003 The determination of activation energy from linear heating rate experiments: A comparison of the accuracy of isoconversion methods *Thermochim Acta* 404 163–76

[258] Henrique M A, Flauzino Neto W P, Silvério H A, Martins D F, Gurgel L V A, Barud H da S, Morais L C de and Pasquini D 2015 Kinetic study of the thermal decomposition of cellulose nanocrystals with different polymorphs, cellulose I and II, extracted from different sources and using different types of acids *Ind Crops Prod* 76 128–40

[259] Vyazovkin S 1997 Advanced isoconversional method *Journal of Thermal Analysis* 49 1493–9

[260] Nawaz A, Mishra R K, Sabbarwal S and Kumar P 2021 Studies of physicochemical characterization and pyrolysis behavior of low-value waste biomass using Thermogravimetric analyzer: evaluation of kinetic and thermodynamic parameters *Bioresour Technol Rep* 16 100858

[261] Kattel K, Park J Y, Xu W, Kim H G, Lee E J, Bony B A, Heo W C, Lee J J, Jin S, Baeck J S, Chang Y, Kim T J, Bae J E, Chae K S and Lee G H 2011 A facile synthesis, in vitro and in vivo MR studies of d-glucuronic acid-coated ultrasmall Ln2O3 (Ln = Eu, Gd, Dy, Ho, and Er) nanoparticles as a new potential MRI contrast agent *ACS Appl Mater Interfaces* 3 3325–34

[262] Ahmad M Y, Ahmad M W, Yue H, Ho S L, Park J A, Jung K H, Cha H, Marasini S, Ghazanfari A, Liu S, Tegafaw T, Chae K S, Chang Y and Lee G H 2020 In vivo positive magnetic resonance imaging applications of poly(methyl vinyl ether-alt-maleic acid)-coated ultra-small paramagnetic gadolinium oxide nanoparticles *Molecules* 25

[263] Aguiar C das D, Coelho Y L, de Paula H M C, Santa Rosa L N, Virtuoso L S, Mendes T A de O, Pires A C dos S and da Silva L H M 2021 Thermodynamic and kinetic insights into the interactions between functionalized CdTe quantum dots and human serum albumin: A surface plasmon resonance approach *Int J Biol Macromol* 184 990–9

[264] Aashima, Pandey S K, Singh S and Mehta S K 2018 Ultrasonication assisted fabrication of L-lysine functionalized gadolinium oxide nanoparticles and its biological acceptability *Ultrason Sonochem* 49 53–62

[265] Nafsin N, Aguiar J A, Aoki T, Thron A M, van Benthem K and Castro R H R 2017 Thermodynamics versus kinetics of grain growth control in nanocrystalline zirconia *Acta Mater* 136 224–34

[266] Bhakta R K, Maharrey S, Stavila V, Highley A, Alam T, Majzoub E and Allendorf M 2012 Thermodynamics and kinetics of NaAlH 4 nanocluster decomposition *Physical Chemistry Chemical Physics* 14 8160–9

[267] Singh B, Singh S and Kumar P 2021 In-depth analyses of kinetics, thermodynamics and solid reaction mechanism for pyrolysis of hazardous petroleum sludge based on isoconversional models for its energy potential *Process Safety and Environmental Protection* 146 85–94

[268] Wallace A F, DeYoreo J J and Dove P M 2009 Kinetics of silica nucleation on carboxyl- and amine-terminated surfaces: Insights for biomineralization *J Am Chem Soc* 131 5244–50

[269] Campi G, Suber L, Righi G, Primitivo L, De Angelis M, Caschera D, Pilloni L, Del Giudice A, Palma A, Satta M, Fortunelli A and Sementa L 2021 Design of a fluorescent and clickable Ag38(SRN3)24nanocluster platform: synthesis, modeling and self-assembling *Nanoscale Adv* 3 2948–60

[270] Chkonia G, Wölk J, Strey R, Wedekind J and Reguera D 2009 Evaluating nucleation rates in direct simulations *Journal of Chemical Physics* 130

[271] Ray S, Bhattacharya T K, Singh V K, Deb D, Ghosh S and Das S 2021 Non-isothermal decomposition kinetics of nano-scale CaCO3 as a function of particle size variation *Ceram Int* 47 858–64

[272] Hu Q, Nielsen M H, Freeman C L, Hamm L M, Tao J, Lee J R I, Han T Y J, Becker U, Harding J H, Dove P M and De Yoreo J J 2012 The thermodynamics of calcite nucleation at organic interfaces: Classical vs. non-classical pathways *Faraday Discuss* 159 509–23

[273] Pitto-Barry A and Barry N P E 2019 Effect of Temperature on the Nucleation and Growth of Precious Metal Nanocrystals *Angewandte Chemie - International Edition* 58 18482–6

[274] Gao X, Huang Z and Fang D 2017 Curvature-dependent interfacial energy and its effects on the elastic properties of nanomaterials *Int J Solids Struct* 113–114 100–7

[275] Nagatsuma Y, Ohno M, Takaki T and Shibuta Y 2021 Bayesian data assimilation of temperature dependence of solid–liquid interfacial properties of nickel *Nanomaterials* 11

[276] França J M P, Nieto De Castro C A and Pádua A A H 2017 Molecular interactions and thermal transport in ionic liquids with carbon nanomaterials *Physical Chemistry Chemical Physics* 19 17075–87

[277] Fizet J, Rivière C, Bridot J L, Charvet N, Louis C, Billotey C, Raccurt M, Morel G, Roux S, Perriat P and Tillement O 2009 Multi-luminescent hybrid gadolinium oxide nanoparticles as potential cell labeling *J Nanosci Nanotechnol* 9 5717–25

[278] Anishur Rahman A T M, Vasilev K and Majewski P 2011 Ultra small Gd2O3 nanoparticles: Absorption and emission properties *J Colloid Interface Sci* 354 592–6

[279] Seo S, Yang H and Holloway P H 2009 Controlled shape growth of Eu- or Tb-doped luminescent Gd2O3 colloidal nanocrystals *J Colloid Interface Sci* 331 236–42

[280] Fang J, Chandrasekharan P, Liu X L, Yang Y, Lv Y B, Yang C T and Ding J 2014 Manipulating the surface coating of ultra-small Gd2O3 nanoparticles for improved T1-weighted MR imaging *Biomaterials* 35 1636–42

[281] Pan Y, Chen W, Yang J, Zheng J, Yang M and Yi C 2018 Facile Synthesis of Gadolinium Chelate-Conjugated Polymer Nanoparticles for Fluorescence/Magnetic Resonance Dual-Modal Imaging *Anal Chem* 90 1992–2000

[282] Lux J, Chan M, Vander Elst L, Schopf E, Mahmoud E, Laurent S and Almutairi A 2013 Metal chelating crosslinkers form nanogels with high chelation stability *J Mater Chem B* 1 6359–64

[283] Shi Y, Pan Y, Zhong J, Yang J, Zheng J, Cheng J, Song R and Yi C 2015 Facile synthesis of gadolinium (III) chelates functionalized carbon quantum dots for fluorescence and magnetic resonance dual-modal bioimaging *Carbon N Y* 93 742–50

[284] Wang Q, Lv L, Ling Z, Wang Y, Liu Y, Li L, Liu G, Shen L, Yan J and Wang Y 2015 Long-circulating iodinated albumin-gadolinium nanoparticles as enhanced magnetic resonance and computed tomography imaging probes for osteosarcoma visualization *Anal Chem* 87 4299–304

[285] Yong Y, Zhou L, Zhang S, Yan L, Gu Z, Zhang G and Zhao Y 2016 Gadolinium polytungstate nanoclusters: A new theranostic with ultrasmall size and versatile properties for dual-modal MR/CT imaging and photothermal therapy/radiotherapy of cancer *NPG Asia Mater* 8

[286] Huang Y, Li L, Zhang D, Gan L, Zhao P, Zhang Y, Zhang Q, Hua M and Jia C 2020 Gadolinium-doped carbon quantum dots loaded magnetite nanoparticles as a bimodal nanoprobe for both fluorescence and magnetic resonance imaging *Magn Reson Imaging* 68 113–20

[287] Pan Y, Yang J, Fang Y, Zheng J, Song R and Yi C 2017 One-pot synthesis of gadolinium-doped carbon quantum dots for high-performance multimodal bioimaging *J Mater Chem B* 5 92–101

[288] Sun S K, Dong L X, Cao Y, Sun H R and Yan X P 2013 Fabrication of multifunctional Gd2O3/Au hybrid nanoprobe via a one-step approach for near-infrared fluorescence and magnetic resonance multimodal imaging in vivo *Anal Chem* 85 8436–41

[289] Majeed S and Shivashankar S A 2014 Rapid, microwave-assisted synthesis of Gd2O3 and Eu:Gd2O3 nanocrystals: Characterization, magnetic, optical and biological studies *J Mater Chem B* 2 5585–93

[290] Xu W, Kattel K, Park J Y, Chang Y, Kim T J and Lee G H 2012 Paramagnetic nanoparticle T 1 and T 2 MRI contrast agents *Physical Chemistry Chemical Physics* 14 12687–700

[291] Ortega-Berlanga B, Betancourt-Mendiola L, Del Angel-Olarte C, Hernández-Adame L, Rosales-Mendoza S and Palestino G 2021 An overview of gadolinium-based oxide and oxysulfide particles: Synthesis, properties, and biomedical applications *Crystals (Basel)* 11 1–34

[292] Selvaraju C, Karthick R and Veerasubam R 2019 The Modification of Structural, Optical and Antibacterial Activity Properties of Rare Earth Gadolinium-Doped ZnO Nanoparticles Prepared by Co-Precipitation Method *J Inorg Organomet Polym Mater* 29 776–82

[293] Dědková K, Kuzníková, Pavelek L, Matějová K, Kupková J, Čech Barabaszová K, Váňa R, Burda J, Vlček J, Cvejn D and Kukutschová J 2017 Daylight induced antibacterial activity of gadolinium oxide, samarium oxide and erbium oxide nanoparticles and their aquatic toxicity *Mater Chem Phys* 197 226–35

[294] Kumar S, Meena V K, Hazari P P and Sharma R K 2017 PEG coated and doxorubicin loaded multimodal Gadolinium oxide nanoparticles for simultaneous drug delivery and imaging applications *Int J Pharm* 527 142–50

[295] Yang H W, Huang C Y, Lin C W, Liu H L, Huang C W, Liao S S, Chen P Y, Lu Y J, Wei K C and Ma C C M 2014 Gadolinium-functionalized nanographene oxide for combined drug and microRNA delivery and magnetic resonance imaging *Biomaterials* 35 6534–42

[296] He K, Li J, Shen Y and Yu Y 2019 PH-Responsive polyelectrolyte coated gadolinium oxide-doped mesoporous silica nanoparticles (Gd2O3@MSNs) for synergistic drug delivery and magnetic resonance imaging enhancement *J Mater Chem B* 7 6840–54

[297] Xu Z, Gao Y, Huang S, Ma P A, Lin J and Fang J 2011 A luminescent and mesoporous core-shell structured Gd2O 3:Eu3+@nSiO2@mSiO2 nanocomposite as a drug carrier *Dalton Transactions* 40 4846–54

[298] Yin L, Zhou J, Li W, Zhang J and Wang L 2019 Yellow fluorescent graphene quantum dots as a phosphor for white tunable light-emitting diodes *RSC Adv* 9 9301–7

[299] Yuan T, Yuan F, Li X, Li Y, Fan L and Yang S 2019 Fluorescence-phosphorescence dual emissive carbon nitride quantum dots show 25% white emission efficiency enabling single-component WLEDs *Chem Sci* 10 9801–6

[300] Feng X and Zhang Y 2019 A simple and green synthesis of carbon quantum dots from coke for white light-emitting devices *RSC Adv* 9 33789–93

[301] Shekhar S, Mahato P, Yadav R, Verma S D and Mukherjee S 2022 White Light Generation through l -Ascorbic Acid-Templated Thermoresponsive Copper Nanoclusters *ACS Sustain Chem Eng* 10 1379–89

[302] Li W, Guo H, Li G, Chi Z, Chen H, Wang L, Liu Y, Chen K, Le M, Han Y, Yin L, Vajtai R, Ajayan P M, Weng Y and Wu M 2020 White luminescent single-crystalline chlorinated graphene quantum dots *Nanoscale Horiz* 5 928–33

[303] Paulo-Mirasol S, Martínez-Ferrero E and Palomares E 2019 Direct white light emission from carbon nanodots (C-dots) in solution processed light emitting diodes *Nanoscale* 11 11315–21

[304] Teunis M B, Lawrence K N, Dutta P, Siegel A P and Sardar R 2016 Pure white-light emitting ultrasmall organic-inorganic hybrid perovskite nanoclusters *Nanoscale* 8 17433–9

[305] Mao L H, Tang W Q, Deng Z Y, Liu S S, Wang C F and Chen S 2014 Facile access to white fluorescent carbon dots toward light-emitting devices *Ind Eng Chem Res* 53 6417–25

[306] Anishur Rahman A T M, Vasilev K and Majewski P 2011 Ultra small Gd2O3 nanoparticles: Absorption and emission properties *J Colloid Interface Sci* 354 592–6

[307] Auzel F 2004 Upconversion and Anti-Stokes Processes with f and d Ions in Solids *Chem Rev* 104 139–73

[308] Haase M and Schäfer H 2011 Upconverting nanoparticles *Angewandte Chemie - International Edition* 50 5808–29

[309] Li J, You J, Dai Y, Shi M, Han C and Xu K 2014 Gadolinium oxide nanoparticles and aptamer-functionalized silver nanoclusters-based multimodal molecular imaging nanoprobe for optical/magnetic resonance cancer cell imaging *Anal Chem* 86 11306–11

[310] Deagostino A, Protti N, Alberti D, Boggio P, Bortolussi S, Altieri S and Crich S G 2016 Insights into the use of gadolinium and gadolinium/boron-based agents in imaging-guided neutron capture therapy applications *Future Med Chem* 8 899–917

[311] Szade J and Neumann M 1996 Photoelectron spectroscopy and magnetism of some gadolinium intermetallic compounds *J Alloys Compd* 236 132–6

[312] Majeed S and Shivashankar S A 2014 Rapid, microwave-assisted synthesis of Gd2O3 and Eu:Gd2O3 nanocrystals: Characterization, magnetic, optical and biological studies *J Mater Chem B* 2 5585–93

[313] Sreeja V, Jayaprabha K N and Joy P A 2015 Water-dispersible ascorbic-acid-coated magnetite nanoparticles for contrast enhancement in MRI *Applied Nanoscience (Switzerland)* 5 435–41

[314] Sahoo K, Khare D, Srikrishna S, Dubey A K and Kumar M 2020 Development of luminescent atacamite nanoclusters for bioimaging and photothermal applications *Nanotechnology* 31

[315] Nelli I, Kaczmarek A M, Locardi F, Caratto V, Costa G A and Van Deun R 2017 Multidoped Ln3+ gadolinium dioxycarbonates as tunable white light emitting phosphors *Dalton Transactions* 46 2785–92

[316] Zaman F, Rooh G, Srisittipokakun N, Ahmad T, Khan I, Shoaib M, Ataullah, Rajagukguk J and Kaewkhao J 2019 Comparative investigations of gadolinium based borate glasses doped with Dy 3+ for white light generations *Solid State Sci* 89 50–6

[317] Erdem M, Örücü H, Cantürk S B and Eryürek G 2021 Upconversion Yb3+/Er3+:Gadolinium Gallium Garnet Nanocrystals for White-Light Emission and Optical Thermometry *ACS Appl Nano Mater* 4 7162–71

[318] Mahajan S V. and Dickerson J H 2007 Synthesis of monodisperse sub-3 nm RE2O3 and Gd 2O3:RE3+ nanocrystals *Nanotechnology* 18

[319] Zhao X, Wang W, Zhang Y, Wu S, Li F and Liu J P 2014 Synthesis and characterization of gadolinium doped cobalt ferrite nanoparticles with enhanced adsorption capability for Congo Red *Chemical Engineering Journal* 250 164–74

[320] Sun S K, Dong L X, Cao Y, Sun H R and Yan X P 2013 Fabrication of multifunctional Gd2O3/Au hybrid nanoprobe via a one-step approach for near-infrared fluorescence and magnetic resonance multimodal imaging in vivo *Anal Chem* 85 8436–41

[321] Jiang X, Yu L, Yao C, Zhang F, Zhang J and Li C 2016 Synthesis and characterization of Gd2O3 hollow microspheres using a template-directed method *Materials* 9

[322] Chen B Bin, Chang S, Lv J, Qian R C and Li D W 2021 Temperature-modulated porous gadolinium micro-networks with hyperchrome-enhanced fluorescence effect *Chemical Engineering Journal* 422 129959

[323] Cheng Y, Lu T, Wang Y, Song Y, Wang S, Lu Q, Yang L, Tan F, Li J and Li N 2019 Glutathione-Mediated Clearable Nanoparticles Based on Ultrasmall Gd 2 O 3 for MSOT / CT / MR Imaging Guided Photothermal / Radio Combination Cancer Therapy

[324] Yuan X, Luo Z, Zhang Q, Zhang X, Zheng Y, Lee J Y and Xie J 2011 Synthesis of highly fluorescent metal (Ag, Au, Pt, and Cu) nanoclusters by electrostatically induced reversible phase transfer *ACS Nano* 5 8800–8

[325] Sabbarwal S, Dubey A K, Pandey M and Kumar M 2020 Synthesis of biocompatible, BSA capped fluorescent CaCO3pre-nucleation nanoclusters for cell imaging applications *J Mater Chem B* 8 5729–44

[326] Bain D, Paramanik B, Sadhu S and Patra A 2015 A study into the role of surface capping on energy transfer in metal cluster-semiconductor nanocomposites *Nanoscale* 7 20697–708

[327] Wang C, Wang C, Xu L, Cheng H, Lin Q and Zhang C 2014 Protein-directed synthesis of pH-responsive red fluorescent copper nanoclusters and their applications in cellular imaging and catalysis *Nanoscale* 6 1775–81

[328] Cai Z, Li H, Wu J, Zhu L, Ma X and Zhang C 2020 Ascorbic acid stabilised copper nanoclusters as fluorescent sensors for detection of quercetin *RSC Adv* 10 8989–93

[329] Li X, Wang G, Chen D and Lu Y 2014 Binding of ascorbic acid and $α$-tocopherol to bovine serum albumin: A comparative study *Mol Biosyst* 10 326–37

[330] Hu L, Sun Y, Li S, Wang X, Hu K, Wang L, Liang X J and Wu Y 2014 Multifunctional carbon dots with high quantum yield for imaging and gene delivery *Carbon N Y* 67 508–13

[331] Zhou X, Zhao G, Tan X, Qian X, Zhang T, Gui J, Yang L and Xie X 2019 Nitrogen-doped carbon dots with high quantum yield for colorimetric and fluorometric detection of ferric ions and in a fluorescent ink *Microchimica Acta* 186

[332] Lee M and Grissom C B 2009 Design, synthesis, and characterization of fluorescent cobalamin analogues with high quantum efficiencies *Org Lett* 11 2499–502

[333] Magde D, Wong R and Seybold P G 2002 Fluorescence Quantum Yields and Their Relation to Lifetimes of Rhodamine 6G and Fluorescein in Nine Solvents: Improved Absolute Standards for Quantum Yields¶ *Photochem Photobiol* 75 327

[334] Wang Q, Lv L, Ling Z, Wang Y, Liu Y, Li L, Liu G, Shen L, Yan J and Wang Y 2015 Long-circulating iodinated albumin-gadolinium nanoparticles as enhanced magnetic resonance and computed tomography imaging probes for osteosarcoma visualization *Anal Chem* 87 4299–304

[335] Online V A 2014 applications in cellular imaging and catalysis † 1775–81

[336] Xu N, Li H W, Yue Y and Wu Y 2016 Synthesis of bovine serum albumin-protected high fluorescence Pt16-nanoclusters and their application to detect sulfide ions in solutions *Nanotechnology* 27

[337] Chatterjee D P, Pakhira M and Nandi A K 2020 Fluorescence in “nonfluorescent” Polymers *ACS Omega* 5 30747–66

[338] Borzova V A, Markossian K A, Chebotareva N A, Kleymenov S Y, Poliansky N B, Muranov K O, Stein-Margolina V A, Shubin V V., Markov D I and Kurganov B I 2016 Kinetics of thermal denaturation andaggregation of bovine serum albumin *PLoS One* 11

[339] Samples S P 2016 A New Indirect Spectrofluorimetric Method for Determination of Ascorbic Acid.

[340] Yong Y, Zhou L, Zhang S, Yan L, Gu Z, Zhang G and Zhao Y 2016 Gadolinium polytungstate nanoclusters: A new theranostic with ultrasmall size and versatile properties for dual-modal MR/CT imaging and photothermal therapy/radiotherapy of cancer *NPG Asia Mater* 8

[341] Wang X Y, Hu Y X, Yang X F, Yin J, Chen Z and Liu S H 2019 Excitation Wavelength-Dependent Nearly Pure White Light-Emitting Crystals from a Single Gold(I)-Containing Complex *Org Lett* 21 9945–9

[342] Zheng W, Sun B, Li Y, Lei T, Wang R and Wu J 2020 Warm white broadband emission and tunable long lifetimes in Yb3+ doped Gd2O3 nanoparticles *Ceram Int* 46 22900–6

[343] Bilir G and Erguzel O 2016 Up-conversion emission properties and unexpected white light emission from Er3+/Yb3+ doped Gd2O3 nanophosphors *Mater Res Express* 3

[344] Li Y, Feng L, Yan W, Hussain I, Su L and Tan B 2019 PVP-templated highly luminescent copper nanoclusters for sensing trinitrophenol and living cell imaging *Nanoscale* 11 1286–94

[345] Yang T Q, Peng B, Shan B Q, Zong Y X, Jiang J G, Wu P and Zhang K 2020 Origin of the photoluminescence of metal nanoclusters: From metal-centered emission to ligand-centered emission *Nanomaterials* 10

[346] Patel A S and Mohanty T 2014 Silver nanoclusters in BSA template: A selective sensor for hydrogen peroxide *J Mater Sci* 49 2136–43

[347] Topală T, Bodoki A, Oprean L and Oprean R 2014 Bovine serum albumin interactions with metal complexes *Clujul Medical* 87 5

[348] Sahoo A K, Banerjee S, Ghosh S S and Chattopadhyay A 2014 Simultaneous RGB emitting Au nanoclusters in chitosan nanoparticles for anticancer gene theranostics *ACS Appl Mater Interfaces* 6 712–24

[349] Chen X, Lv G, Zhang J, Tang S, Yan Y, Wu Z, Su J and Wei J 2014 Preparation and properties of bsa-loaded microspheres based on multi-(amino acid) copolymer for protein delivery *Int J Nanomedicine* 9 1957–65

[350] Sabaa M W, Hanna D H, Abu Elella M H and Mohamed R R 2019 Encapsulation of bovine serum albumin within novel xanthan gum based hydrogel for protein delivery *Materials Science and Engineering C* 94 1044–55

[351] Abu Elella M H, Hanna D H, Mohamed R R and Sabaa M W 2022 Synthesis of xanthan gum/trimethyl chitosan interpolyelectrolyte complex as pH-sensitive protein carrier *Polymer Bulletin* 79 2501–22

[352] Wang Z, Dong Y, Li H, Zhao Z, Bin Wu H, Hao C, Liu S, Qiu J and Lou X W D 2014 Enhancing lithium-sulphur battery performance by strongly binding the discharge products on amino-functionalized reduced graphene oxide *Nat Commun* 5

[353] Dave K, Park K H and Dhayal M 2015 Two-step process for programmable removal of oxygen functionalities of graphene oxide: functional, structural and electrical characteristics *RSC Adv* 5 95657–65

[354] Jeon S, Ko J W and Ko W B 2021 Synthesis of gd2 o3 nanoparticles and their photocatalytic activity for degradation of azo dyes *Catalysts* 11

[355] Premlatha S, Selvarani K and Ramesh Bapu G N K 2018 Facile Electrodeposition of Hierarchical Co-Gd2O3 Nanocomposites for Highly Selective and Sensitive Electrochemical Sensing of L–Cysteine *ChemistrySelect* 3 2665–74

[356] Abdeldayem H M, Faiz M, Abdel-Samad H S and Hassan S A 2015 Rare earth oxides doped NiO/γ-Al2O3 catalyst for oxidative dehydrogenation of cyclohexane *Journal of Rare Earths* 33 611–8

[357] Artemenko A, Shchukarev A, Štenclová P, Wagberg T, Segervald J, Jia X and Kromka A 2021 Reference XPS spectra of amino acids *IOP Conf Ser Mater Sci Eng* 1050

[358] Ahrén M, Selegård L, Söderlind F, Linares M, Kauczor J, Norman P, Käll P O and Uvdal K 2012 A simple polyol-free synthesis route to Gd2O3 nanoparticles for MRI applications: An experimental and theoretical study *Journal of Nanoparticle Research* 14

[359] Zhou J P, Chai C L, Yang S Y, Liu Z K, Song S L, Li Y L and Chen N F 2004 Properties of high k gate dielectric gadolinium oxide deposited on Si (1 0 0) by dual ion beam deposition (DIBD) *J Cryst Growth* 270 21–9

[360] Raiser D and Deville J P 1991 Study of XPS photoemission of some gadolinium compounds *J Electron Spectros Relat Phenomena* 57 91–7

[361] Sarparast M, Noori A, Ilkhani H, Bathaie S Z, El-Kady M F, Wang L J, Pham H, Marsh K L, Kaner R B and Mousavi M F 2016 Cadmium nanoclusters in a protein matrix: Synthesis, characterization, and application in targeted drug delivery and cellular imaging *Nano Res* 9 3229–46

[362] Cui D, Huang P, Li Z and Hu H 2010 Synthesis and characterization of bovine serum albumin-conjugated copper sulfide nanocomposites *J Nanomater* 2010

[363] Song L, Du P, Jiang Q, Cao H and Xiong J 2014 یدنب هجنسو تخاس ، زتنس دنیآرف وترپ یزاسراکشآ X 150 رفسفونان (GOS) + Tb 3 : Gd 2 O 2 S) م یسررب رد هدافتسادرو 50–4

[364] Alhazmi H A 2019 FT-IR spectroscopy for the identification of binding sites and measurements of the binding interactions of important metal ions with bovine serum albumin *Sci Pharm* 87

[365] Wu Z and Jin R 2010 On the ligand's role in the fluorescence of gold nanoclusters *Nano Lett* 10 2568–73

[366] Xu Y, Sherwood J, Qin Y, Crowley D, Bonizzoni M and Bao Y 2014 The role of protein characteristics in the formation and fluorescence of Au nanoclusters *Nanoscale* 6 1515–24

[367] Hazarika S and Mohanta D 2013 Production and optoelectronic response of Tb3+ activated gadolinium oxide nanocrystalline phosphors *EPJ Applied Physics* 62 1–5

[368] Zatsepin A F and Review A 2017 Optical properties and energy parameters of Gd 2 O 3 and Gd 2 O 3 : Er nanoparticles Optical properties and energy parameters of Gd 2 O 3 and Gd 2 O 3 : Er nanoparticles 2–6

[369] Manigandan R, Giribabu K, Suresh R, Vijayalakshmi L, Stephen A and Narayanan V 2013 Structural, optical and magnetic properties of gadolinium sesquioxide nanobars synthesized via thermal decomposition of gadolinium oxalate *Mater Res Bull* 48 4210–5

[370] Coil I, Prepared H, Fluorescent H and Sensor E 2014 Electronic Supplementary Information Induction Coil Heater Prepared Highly Fluorescent Carbon Dots as Invisible Ink and Explosive Sensor 1–14

[371] Fizet J, Rivière C, Bridot J L, Charvet N, Louis C, Billotey C, Raccurt M, Morel G, Roux S, Perriat P and Tillement O 2009 Multi-luminescent hybrid gadolinium oxide nanoparticles as potential cell labeling *J Nanosci Nanotechnol* 9 5717–25

[372] Li Q and Jun Y S 2018 The apparent activation energy and pre-exponential kinetic factor for heterogeneous calcium carbonate nucleation on quartz *Commun Chem* 1 1–9

[373] Joop H and Sefcik J 2020 *The Handbook of Continuous Crystallization* (The Royal Society of Chemistry)

[374] Henrique M A, Flauzino Neto W P, Silvério H A, Martins D F, Gurgel L V A, Barud H da S, de Morais L C and Pasquini D 2015 Kinetic study of the thermal decomposition of cellulose nanocrystals with different polymorphs, cellulose I and II, extracted from different sources and using different types of acids *Ind Crops Prod* 76 128–40

[375] Carpenter J E and Grünwald M 2021 Pre-Nucleation Clusters Predict Crystal Structures in Models of Chiral Molecules *J Am Chem Soc* 143 21580–93

[376] Oyelaran O, Novet T, Johnson C D and Johnson D C 1996 Controlling solid-state reaction pathways: Composition dependence in the nucleation energy of InSe *J Am Chem Soc* 118 2422–6

[377] Ihli J, Wong W C, Noel E H, Kim Y Y, Kulak A N, Christenson H K, Duer M J and Meldrum F C 2014 Dehydration and crystallization of amorphous calcium carbonate in solution and in air *Nat Commun* 5 1–10

[378] Oyelaran O, Novet T, Johnson C D and Johnson D C 1996 Controlling solid-state reaction pathways: Composition dependence in the nucleation energy of InSe *J Am Chem Soc* 118 2422–6

[379] Koga N 2018 *Physico-Geometric Approach to the Kinetics of Overlapping Solid-State Reactions* vol 6 (Elsevier B.V.)

[380] Koga N and Tanaka H 1992 Effect of sample mass on the kinetics of thermal decomposition of a solid *Thermochim Acta* 209 127–34

[381] Chaudhary S, Kumar S and Mehta S K 2015 Glycol modified gadolinium oxide nanoparticles as a potential template for selective and sensitive detection of 4-nitrophenol *J Mater Chem C Mater* 3 8824–33

[382] Perevalov T V, Dolbak A E, Shvets V A, Gritsenko V A, Asanova T I and Erenburg S B 2014 Atomic and electronic structure of gadolinium oxide *EPJ Applied Physics* 65 3–6

[383] Relaxivity L, Particle O, Park J Y, Baek M J, Choi E S, Woo S, Kim J H, Kim T J, Jung J C, Chae S, Chang Y and Lee G H 2009 Oxide Nanoparticles as Advanced T 1 *ACS Nano* 3 3663–9

[384] Aguiar C das D, Coelho Y L, de Paula H M C, Santa Rosa L N, Virtuoso L S, Mendes T A de O, Pires A C dos S and da Silva L H M 2021 Thermodynamic and kinetic insights into the interactions between functionalized CdTe quantum dots and human serum albumin: A surface plasmon resonance approach *Int J Biol Macromol* 184 990–9

[385] Mishra G and Bhaskar T 2014 Non isothermal model free kinetics for pyrolysis of rice straw *Bioresour Technol* 169 614–21

[386] Najarnia F, Ahmadpoor F, Sahebian S, Johnson J A, Kamali S and Shojaosadati S A 2022 Thermal decomposition kinetic study of Fe5C2 nanoparticles *Journal of Physics and Chemistry of Solids* 161 110436

[387] Wanjun T, Cunxin W and Donghua C 2006 An investigation of the pyrolysis kinetics of some aliphatic amino acids *J Anal Appl Pyrolysis* 75 49–53

[388] Flynn J H 1997 The “temperature integral” - Its use and abuse *Thermochim Acta* 300 83–92

[389] Kissinger H E 1957 Reaction Kinetics in Differential Thermal Analysis *Anal Chem* 29 1702–6

[390] Vyazovkin S 2001 Modification of the Integral Isoconversional Method to Account for Variation in the Activation Energy *J Comput Chem* 22 178–83

[391] Kovinchuk I, Haiuk N, Lazzara G, Cavallaro G and Sokolsky G 2023 Enhanced photocatalytic degradation of PE film by anatase/γ-MnO2 *Polym Degrad Stab* 210 110295

[392] Zabihi O and Khodabandeh A 2013 Understanding of thermal/thermo-oxidative degradation kinetics of polythiophene nanoparticles *J Therm Anal Calorim* 112 1507–13

[393] Jelić D, Liavitskaya T and Vyazovkin S 2019 Thermal stability of indomethacin increases with the amount of polyvinylpyrrolidone in solid dispersion *Thermochim Acta* 676 172–6

[394] Calvino M M, Lisuzzo L, Cavallaro G, Lazzara G and Milioto S 2021 Non-isothermal thermogravimetry as an accelerated tool for the shelf-life prediction of paracetamol formulations *Thermochim Acta* 700 178940

[395] Chen Y and Wang Q 2007 Thermal oxidative degradation kinetics of flame-retarded polypropylene with intumescent flame-retardant master batches in situ prepared in twin-screw extruder *Polym Degrad Stab* 92 280–91

[396] Tiptipakorn S, Damrongsakkul S, Ando S, Hemvichian K and Rimdusit S 2007 Thermal degradation behaviors of polybenzoxazine and silicon-containing polyimide blends *Polym Degrad Stab* 92 1265–78

[397] Starink M J 2003 The determination of activation energy from linear heating rate experiments: A comparison of the accuracy of isoconversion methods *Thermochim Acta* 404 163–76

[398] Kissinger H E 1957 Reaction Kinetics in Differential Thermal Analysis *Anal Chem* 29 1702–6

[399] Singh B, Singh S and Kumar P 2021 In-depth analyses of kinetics, thermodynamics and solid reaction mechanism for pyrolysis of hazardous petroleum sludge based on isoconversional models for its energy potential *Process Safety and Environmental Protection* 146 85–94

[400] Tang W, Liu Y, Zhang H and Wang C 2003 New approximate formula for Arrhenius temperature integral *Thermochim Acta* 408 39–43

[401] Vyazovkin S, Burnham A K, Criado J M, Pérez-Maqueda L A, Popescu C and Sbirrazzuoli N 2011 ICTAC Kinetics Committee recommendations for performing kinetic computations on thermal analysis data *Thermochim Acta* 520 1–19

[402] Vyazovkin S 2001 Modification of the Integral Isoconversional Method to Account for Variation in the Activation Energy *J Comput Chem* 22 178–83

[403] Pérez-Maqueda L A and Criado J M 2000 Accuracy of Senum and Yang's approximations to the Arrhenius integral *J Therm Anal Calorim* 60 909–15

[404] Dhyani V, Kumar J and Bhaskar T 2017 Thermal decomposition kinetics of sorghum straw via thermogravimetric analysis *Bioresour Technol* 245 1122–9

[405] Bhardwaj G, Kumar M, Mishra P K and Upadhyay S N 2021 Kinetic analysis of the slow pyrolysis of paper wastes *Biomass Convers Biorefin*

[406] Nawaz A, Mishra R K, Sabbarwal S and Kumar P 2021 Studies of physicochemical characterization and pyrolysis behavior of low-value waste biomass using Thermogravimetric analyzer: evaluation of kinetic and thermodynamic parameters *Bioresour Technol Rep* 16 100858

[407] Singh S, Prasad Chakraborty J and Kumar Mondal M 2020 Intrinsic kinetics, thermodynamic parameters and reaction mechanism of non-isothermal degradation of torrefied Acacia nilotica using isoconversional methods *Fuel* 259 116263

[408] Srivastava P, Sabbarwal S, Verma V K and Kumar M 2023 A novel approach for determination of nucleation rates and interfacial energy of metallic magnesium nanoclusters at high temperature using non-isothermal TGA models *Chem Eng Sci* 265 118223

[409] Hu Q, Nielsen M H, Freeman C L, Hamm L M, Tao J, Lee J R I, Han T Y J, Becker U, Harding J H, Dove P M and De Yoreo J J 2012 The thermodynamics of calcite nucleation at organic interfaces: Classical vs. non-classical pathways *Faraday Discuss* 159 509–23

[410] Vehkamäki H 2006 *Classical nucleation theory in multicomponent systems*

[411] Lindenberg C and Mazzotti M 2009 Effect of temperature on the nucleation kinetics of α l-glutamic acid *J Cryst Growth* 311 1178–84

[412] Ghosh R, Sahoo A K, Ghosh S S, Paul A and Chattopadhyay A 2014 Blue-emitting copper nanoclusters synthesized in the presence of lysozyme as candidates for cell labeling *ACS Appl Mater Interfaces* 6 3822–8

[413] Yang Z, Yang L, Dai B, Lei P, Guo S, Wang P, Wang Q, Ding Y, Zhang Y, Han J and Zhu J 2019 Evolution of microstructures and optical properties of gadolinium oxide with oxygen flow rate and annealing temperature *Journal of Rare Earths* 37 410–5

[414] Shu C Y, Gan L H, Wang C R, Pei X L and Han H Bin 2006 Synthesis and characterization of a new water-soluble endohedral metallofullerene for MRI contrast agents *Carbon N Y* 44 496–500

[415] Wang Y, Yu H, Bi M, Shen X, Li T, Qin S and Yao S 2022 Gadolinium oxide nanorods decorated Ketjen black@sulfur composites as functional catalyzing polysulfides conversion in lithium/sulfur batteries *Int J Energy Res* 16050–60

[416] Li M, Wang Y, Zheng Y, Fu G, Sun D, Li Y, Tang Y and Ma T 2020 Gadolinium-Induced Valence Structure Engineering for Enhanced Oxygen Electrocatalysis *Adv Energy Mater* 10 1–10

[417] Li J, Wu C, Hou P, Zhang M and Xu K 2018 One-pot preparation of hydrophilic manganese oxide nanoparticles as T1 nano-contrast agent for molecular magnetic resonance imaging of renal carcinoma in vitro and in vivo *Biosens Bioelectron* 102 1–8

[418] Khawam A and Flanagan D R 2006 Solid-state kinetic models: Basics and mathematical fundamentals *Journal of Physical Chemistry B* 110 17315–28

[419] Merabia S, Shenogin S, Joly L, Keblinski P and Barrat J L 2009 Heat transfer from nanoparticles: A corresponding state analysis *Proc Natl Acad Sci U S A* 106 15113–8

[420] Yuan X, He T, Cao H and Yuan Q 2017 Cattle manure pyrolysis process: Kinetic and thermodynamic analysis with isoconversional methods *Renew Energy* 107 489–96

[421] Wang R, Xie C, Zeng L and Xu H 2019 Thermal decomposition behavior and kinetics of nanocomposites at low-modified ZnO content *RSC Adv* 9 790–800

[422] Dhyani V, Kumar J and Bhaskar T 2017 Thermal decomposition kinetics of sorghum straw via thermogravimetric analysis *Bioresour Technol* 245 1122–9

[423] Palmay P, Mora M, Barzallo D and Bruno J C 2021 Determination of thermodynamic parameters of polylactic acid by thermogravimetry under pyrolysis conditions *Applied Sciences (Switzerland)* 11

[424] Fernandez-Martinez A, Hu Y, Lee B, Jun Y S and Waychunas G A 2013 In situ determination of interfacial energies between heterogeneously nucleated CaCO3 and quartz substrates: Thermodynamics of CO 2 mineral trapping *Environ Sci Technol* 47 102–9

[425] Hamm L M, Giuffre A J, Han N, Tao J, Wang D, De Yoreo J J and Dove P M 2014 Reconciling disparate views of template-directed nucleation through measurement of calcite nucleation kinetics and binding energies *Proc Natl Acad Sci U S A* 111 1304–9

[426] Wallace A F, DeYoreo J J and Dove P M 2009 Kinetics of silica nucleation on carboxyl- and amine-terminated surfaces: Insights for biomineralization *J Am Chem Soc* 131 5244–50

[427] Sounart T L, Liu J, Voigt J A, Huo M, Spoerke E D and McKenzie B 2007 Secondary nucleation and growth of ZnO *J Am Chem Soc* 129 15786–93

[428] Jha R, Diercks D R, Chakraborti N, Stebner A P and Ciobanu C V 2019 Interfacial energy of copper clusters in Fe-Si-B-Nb-Cu alloys *Scr Mater* 162 331–4

[429] Gozzi D, Tomellini M, Lazzarini L and Latini A 2010 High-temperature determination of surface free energy of copper nanoparticles *Journal of Physical Chemistry C* 114 12117–24

[430] Sounart T L, Liu J, Voigt J A, Huo M, Spoerke E D and McKenzie B 2007 Secondary nucleation and growth of ZnO *J Am Chem Soc* 129 15786–93

[431] Li J, You J, Dai Y, Shi M, Han C and Xu K 2014 Gadolinium oxide nanoparticles and aptamer-functionalized silver nanoclusters-based multimodal molecular imaging nanoprobe for optical/magnetic resonance cancer cell imaging *Anal Chem* 86 11306–11

[432] Wolfbeis O S 2015 An overview of nanoparticles commonly used in fluorescent bioimaging *Chem Soc Rev* 44 4743–68

[433] Brune N, Mues B, Buhl E M, Hintzen K-W, Jockenhoevel S, Cornelissen C G, Slabu I and Thiebes A L 2023 Dual Labeling of Primary Cells with Fluorescent Gadolinium Oxide Nanoparticles *Nanomaterials* 13 1869

[434] Gossuin Y, Hocq A, Vuong Q L, Disch S, Hermann R P and Gillis P 2008 Physico-chemical and NMR relaxometric characterization of gadolinium hydroxide and dysprosium oxide nanoparticles *Nanotechnology* 19

[435] Fatima A, Ahmad M W, Al Saidi A K A, Choudhury A, Chang Y and Lee G H 2021 Recent advances in gadolinium based contrast agents for bioimaging applications *Nanomaterials* 11 1–23

[436] Bazzi R, Flores M A, Louis C, Lebbou K, Zhang W, Dujardin C, Roux S, Mercier B, Ledoux G, Bernstein E, Perriat P and Tillement O 2004 Synthesis and properties of europium-based phosphors on the nanometer scale: Eu2O3, Gd2O3:Eu, and Y 2O3:Eu *J Colloid Interface Sci* 273 191–7

[437] Söderlind F, Pedersen H, Petoral R M, Käll P O and Uvdal K 2005 Synthesis and characterisation of Gd2O3 nanocrystals functionalised by organic acids *J Colloid Interface Sci* 288 140–8

[438] Relaxivity L, Particle O, Park J Y, Baek M J, Choi E S, Woo S, Kim J H, Kim T J, Jung J C, Chae S, Chang Y and Lee G H 2009 Oxide Nanoparticles as Advanced T 1 *ACS Nano* 3 3663–9

[439] Sahoo A K, Banerjee S, Ghosh S S and Chattopadhyay A 2014 Simultaneous RGB emitting Au nanoclusters in chitosan nanoparticles for anticancer gene theranostics *ACS Appl Mater Interfaces* 6 712–24

[440] Nagpal K, Singh S K and Mishra D N 2010 Chitosan nanoparticles: A promising system in novel drug delivery *Chem Pharm Bull (Tokyo)* 58 1423–30

[441] Bulmer C, Margaritis A and Xenocostas A 2012 Production and characterization of novel chitosan nanoparticles for controlled release of rHu-Erythropoietin *Biochem Eng J* 68 61–9

[442] Das S, Goswami P, Verma V K, Indurthi H K, Kumar M, Koch B and Sharma D K 2023 Rapid access to 7-substituted cycloalkylamino and alkylamino analogues of 4-methylcoumarin reveals surprising emitters *Dyes and Pigments* 217 111407

[443] Li Y, Feng L, Yan W, Hussain I, Su L and Tan B 2019 PVP-templated highly luminescent copper nanoclusters for sensing trinitrophenol and living cell imaging *Nanoscale* 11 1286–94

[444] Srivastava P, Verma V K and Sabbarwal S soluble metallic magnesium nanoclusters for bioimaging applications

[445] Kumar Verma V, Srivastava P, Sabbarwal S, Singh M, Koch B and Kumar M 2022 White Light Emitting Gadolinium Oxide Nanoclusters for In-vitro Bio-imaging *ChemistrySelect* 7

[446] Sabbarwal S, Dubey A K, Pandey M and Kumar M 2020 Synthesis of biocompatible, BSA capped fluorescent CaCO3pre-nucleation nanoclusters for cell imaging applications *J Mater Chem B* 8 5729–44

[447] Sahoo A K, Banerjee S, Ghosh S S and Chattopadhyay A 2014 Simultaneous RGB emitting Au nanoclusters in chitosan nanoparticles for anticancer gene theranostics *ACS Appl Mater Interfaces* 6 712–24

[448] Saeid Y A and Ateia E E 2022 Efficient removal of Pb (II) from water solution using CaFe2−x−yGdxSmyO4 ferrite nanoparticles *Appl Phys A Mater Sci Process* 128

[449] Park S J, Park J Y, Yang H K, Moon B K and Oh J 2018 Biocompatible sphere, square prism and hexagonal rod Gd 2 O 3 :Eu 3+ @SiO 2 nanoparticles: The effect of morphology on multi-modal imaging *Colloids Surf B Biointerfaces* 172 224–32

[450] Transactions E C S and Society T E 2015 ~1.2 - 1.4 V and reset voltage, V 66 287–93

[451] Zatsepin D A, Boukhvalov D W, Zatsepin A F, Kuznetsova Y A, Mashkovtsev M A, Rychkov V N, Shur V Y, Esin A A and Kurmaev E Z 2018 Electronic structure, charge transfer, and intrinsic luminescence of gadolinium oxide nanoparticles: Experiment and theory *Appl Surf Sci* 436 697–707

[452] Yang S, Gao H, Wang Y, Xin S, He Y, Wang Y and Zeng W 2013 A simple way to synthesize well-dispersed Gd2O3 nanoparticles onto reduced graphene oxide sheets *Mater Res Bull* 48 37–40

[453] Gayathri T, Sundaram N M and Kumar R A 2015 Gadolinium oxide nanoparticles for Magnetic Resonance Imaging and cancer theranostics *Journal of Bionanoscience* 9 409–23

[454] Alhazmi H A 2019 FT-IR spectroscopy for the identification of binding sites and measurements of the binding interactions of important metal ions with bovine serum albumin *Sci Pharm* 87

[455] Muzzarelli R A A, Tanfani F and Emanuelli M 1984 Chelating derivatives of chitosan obtained by reaction with ascorbic acid *Carbohydr Polym* 4 137–51

[456] Zain N M, Stapley A G F and Shama G 2014 Green synthesis of silver and copper nanoparticles using ascorbic acid and chitosan for antimicrobial applications *Carbohydr Polym* 112 195–202

[457] Arab C, El Kurdi R and Patra D 2021 Chitosan coated zinc curcumin oxide nanoparticles for the determination of ascorbic acid *J Mol Liq* 328 115504

[458] Elansary M, Belaiche M, Mouhib Y, Lemine O M, Bentarhlia N and Bsoul I 2023 Novel biocompatible nanomaterial for biomedical application: Structural, morphological, magnetic, and in vivo toxicity investigations *Ceram Int* 49 4551–70

[459] Zhang C, Jin J, Zhao J, Jiang W and Yin J 2013 Functionalized polypropylene non-woven fabric membrane with bovine serum albumin and its hemocompatibility enhancement *Colloids Surf B Biointerfaces* 102 45–52

[460] Sun S K, Dong L X, Cao Y, Sun H R and Yan X P 2013 Fabrication of multifunctional Gd2O3/Au hybrid nanoprobe via a one-step approach for near-infrared fluorescence and magnetic resonance multimodal imaging in vivo *Anal Chem* 85 8436–41

[461] Huang H, Liu F, Chen S, Zhao Q, Liao B, Long Y, Zeng Y and Xia X 2013 Enhanced fluorescence of chitosan based on size change of micelles and application to directly selective detecting Fe3+ in human serum *Biosens Bioelectron* 42 539–44

[462] Hagberg G E and Scheffler K 2013 Effect of r1 and r2 relaxivity of gadolinium-based contrast agents on the T1-weighted MR signal at increasing magnetic field strengths *Contrast Media Mol Imaging* 8 456–65

Appendix A

Table A1. Pre-exponential kinetic factor (A_a) computed from KAS-derived Equation at 10ºC/min.

Conversions	$A\ (min^{-1})$	$A\ (nuclei\ \mu m^{-2}\ min^{-1})$
0.05	**38820.15566**	**4.22182E+19**
0.1	**6.06412E+13**	**6.59493E+28**
0.15	**2.43484E+11**	**2.64797E+26**
0.2	**9.99855E+12**	**1.08738E+28**
0.25	**7.34E+14**	**7.98E+29**
0.3	**4.38179E+13**	**4.77E+28**
0.35	**9.06E+14**	**9.85E+29**
0.4	**7.11E+15**	**7.73E+30**
0.45	**4.17E+16**	**4.54E+31**
0.5	**2.92E+16**	**3.17E+31**
0.55	**1.61E+16**	**1.75E+31**
0.6	**1.26E+14**	**1.37E+29**
0.65	**5.64E+16**	**6.13E+31**
0.7	**1.27E+16**	**1.38E+31**
0.75	**8.73E+13**	**9.49E+28**
0.8	**2.44E+15**	**2.65E+30**
0.85	**2.35E+14**	**2.55E+29**
0.9	**2.79471E+14**	**3.0393E+29**
0.95	**1.22E+15**	**1.33E+30**

Table A2. Nucleation Rate calculated by Kinetic and Thermodynamic barriers required for Random Nucleation within the Gd_2O_3 matrix concerning Temperature.

T(K)	J_n ($nuclei\ \mu m^{-2}\ min^{-1}$) 10^0C/min	T(K)	J_n ($nuclei\ \mu m^{-2}\ min^{-1}$) 15^0C/min	T(K)	J_n ($nuclei\ \mu m^{-2}\ min^{-1}$) 20^0C/min
562.2	1.735	**569.2**	3.90	**573.17**	4.40
572.18	5.19	**579.18**	11.33	**584.22**	14.40
579.22	13.0	**586.15**	27.7	**590.18**	30.74
585.15	28.4	**592.21**	60.29	**596.29**	65.98
591.17	62.79	**598.26**	131.52	**602.2**	139.11
597.2	120.92	**604.16**	245.65	**608.26**	263.11
603.17	229.29	**610.2**	462.40	**614.19**	487.71
612.23	388.94	**619.17**	763.97	**623.24**	829.68
624.18	2460.05	**631.15**	4679.30	**636.21**	5329.44
640.18	10393.64	**647.2**	19226.88	**653.22**	23652.14
663.15	39960.5	**671.19**	77796.54	**677.19**	94565.03
685.15	458854.8	**694.18**	922005.8	**700.19**	1071619
718.16	3696449	**728.23**	7516334	**735.15**	9092955
781.17	2.7×10^8	**794.23**	5.88×10^8	**800.18**	6.28×10^8
857.23	3.3×10^{10}	**870.24**	6.36×10^{10}	**881.23**	8.22×10^{10}

Table A2.1

Nucleation rate Vs. Temperatures			
	10 ˚C/min	**15 ˚C/min**	**20 ˚C/min**
A1	0.49383	0.017077	1.35545
t1	15.775 ± 0.0044	11.378 ± 3.1330	16.628 ± 0.0054

A1 and t1 are the exponential functions constant for the best-fitted plot between nucleation rate and Temperature.

Table A2.2

Nucleation rate Vs. Conversions			
	10 ˚C/min	**15 ˚C/min**	**20 ˚C/min**
A1	0.03231	0.11967	0.07705
t1	0.01868 ± 0.135	0.01537 ± 0.407	0.01866 ± 0.136
A2	-0.21021	-0.19791	-0.50477
t2	0.0202 ± 0.161	0.0157 ± 0.432	0.0201 ± 0.162

A1, A2, t1, and t2 are exponential function constants for the best-fitted plot between nucleation rate and conversions.

Table A3. The value of Interfacial energy is calculated by Thermodynamic barriers within the Gd_2O_3 matrix with Temperature.

T(K)	ϒ (mJ/m^2)-10˚C/min	T(K)	ϒ (mJ/m^2)-15˚C/min	T(K)	ϒ (mJ/m^2)-20˚C/min
503.17	49.31	**510.17**	49.77	**513.28**	49.89
528.19	44.79	**535.22**	45.18	**540.31**	45.37
549.23	50.61	**556.19**	51.03	**560.28**	51.37
562.2	51.33	**569.2**	51.75	**573.17**	52.08
572.18	51.98	**579.18**	52.40	**584.22**	52.79
579.22	52.36	**586.15**	52.77	**590.18**	53.10
585.15	52.68	**592.21**	53.10	**596.29**	53.43
591.17	53.0	**598.26**	53.44	**602.2**	53.76
597.2	53.38	**604.16**	53.79	**608.26**	54.12
603.17	53.75	**610.2**	54.16	**614.19**	54.45
612.23	54.36	**619.17**	54.77	**623.24**	55.10
624.18	54.97	**631.15**	55.37	**636.21**	55.76
640.18	55.93	**647.2**	56.33	**653.22**	56.77
663.15	57.34	**671.19**	57.80	**677.19**	58.24
685.15	58.54	**694.18**	59.05	**700.19**	59.49
718.16	60.45	**728.23**	61.01	**735.15**	61.50
781.17	63.93	**794.23**	64.64	**800.18**	65.07
857.23	67.99	**870.24**	68.67	**881.23**	69.37

Table A3.1:

Interfacial Vs Temperature			
	10 °C/min	**15 °C/min**	**20 °C/min**
a	18.451 ± 3.997E-15	18.611 ± 2.029E-15	18.742 ± 5.009E-15
b	0.058 ± 6.289E-18	0.058 ± 3.151E-18	0.058 ± 7.709E-18

a and b are linear function constants for the best-fitted plot between interfacial and Temperature.

Table A3.2:

Interfacial Vs Conversions			
	10 °C/min	**15 °C/min**	**20 °C/min**
Intercept (I)	51.893 ± 8.437E-15	52.454 ± 1.352E-14	52.895 ± 9.907E-16
b1	-6.603 ± 3.478E-14	-7.330 ± 5.574E-14	-7.914 ± 4.084E-15
b2	18.697 ± 3.270E-14	19.512 ± 5.242E-14	20.266 ± 3.840E-15

I, b1, and b2 are polynomial function constants for the fitted plot between interfacial energy and conversion.

Table A4: Mechanism for f (α) and I (α) functions for some common mechanisms operating in solid-state reactions.

Mechanism (Nucleation model)	**I(α)**	**g(α)**
A1, sigmoidal rate equation (Avarami equation)	$[-\ln(1-\alpha)]^{2/3}$	$(3/2)\,(1-\alpha)[-\ln(1-\alpha)]^{1/3}$
A2, sigmoidal rate equation (Avarami equation)	$[-\ln(1-\alpha)]^{1/2}$	$2(1-\alpha)[-\ln(1-\alpha)]^{1/2}$
A3, sigmoidal rate equation (Avarami equation)	$[-\ln(1-\alpha)]^{1/3}$	$3(1-\alpha)[-\ln(1-\alpha)]^{2/3}$
A4, sigmoidal rate equation (Avarami equation)	$[-\ln(1-\alpha)]^{1/4}$	$4(1-\alpha)[-\ln(1-\alpha)]^{3/4}$
F1, sigmoidal rate equation (Prout-Tompkins)	$\ln[\alpha/(1-\alpha)]$	$\alpha(1-\alpha)$
F2, sigmoidal rate equation (Contracting area)	$1-(1-\alpha)^{1/2}$	$2(1-\alpha)^{1/2}$
F3, sigmoidal rate equation (Contracting volume)	$1-(1-\alpha)^{1/3}$	$3(1-\alpha)^{2/3}$
F4, sigmoidal rate equation (Random nucleation (1))	$1/(1-\alpha)$	$(1-\alpha)^2$
F4, sigmoidal rate equation (Random nucleation (2))	$1/(1-\alpha)^2$	$(1-\alpha)^3/2$
R1, Reaction rate models (First order)	$-\ln(1-\alpha)$	$1-\alpha$
R1, Reaction rate models (Second order)	$(1-\alpha)^{-1}-1$	$(1-\alpha)^2$
R1, Reaction rate models (Third order)	$[(1-\alpha)^{-2}-1]/2$	$(1-\alpha)^3$
R1, Reaction rate models (Fourth order)	$2[(1-\alpha)^{-1/2}-1]$	$(1-\alpha)^{3/2}$
D1, Diffusion models (1 dimensional)	α^2	$1/2\alpha$
D2, Diffusion models (2 dimensional-Valensi)	$(1-\alpha)\ln(1-\alpha)+\alpha$	$[-\ln(1-\alpha)]^{-1}$

D3, Diffusion models (3 dimensional-Jander))	$[1-(1-\alpha)^{1/3}]^2$	$(3/2)(1-\alpha)^{2/3} / [1-(1-\alpha)^{1/3}]$
D4, Diffusion models (4 dimensional-Ginstling))	$1-2\alpha/3-(1-\alpha)^{2/3}$	$(3/2)/[(1-\alpha)^{-1/3} - 1]$
P2, Power Law	$\alpha^{3/2}$	$(2/3)\alpha^{-1/2}$
P3, Power Law	$\alpha^{1/2}$	$2\alpha^{1/2}$
P4, Power Law	$\alpha^{1/3}$	$3\alpha^{2/3}$
P5, Power Law	$\alpha^{1/4}$	$4\alpha^{3/4}$

Section A1:

The size range of ultra-small gadolinium oxide nanoclusters during nucleation is being calculated at all three heating rates using equation 1, and according to Temperature, the sizes are listed below in Table a5:

Table A5. Variation in size of prepared Gd_2O_3 with the Temperature

Heating rate @ 10°C/min		**Heating rate @ 15°C/min**		**Heating rate @ 20°C/min**	
Temperature (K)	**Size (nm)**	**Temperature (K)**	**Size (nm)**	**Temperature (K)**	**Size (nm)**
503.17	1.15	510.17	1.14	513.28	1.14
528.19	0.99	535.22	0.99	540.31	0.98
549.23	1.08	556.19	1.08	560.28	1.07
562.2	1.07	569.2	1.07	573.17	1.06
572.18	1.06	579.18	1.06	584.22	1.06
579.22	1.06	586.15	1.06	590.18	1.05
585.15	1.06	592.21	1.05	596.29	1.05
591.17	1.05	598.26	1.05	602.2	1.05
597.2	1.05	604.16	1.04	608.26	1.04
603.17	1.04	610.2	1.04	614.19	1.04
612.23	1.04	619.17	1.04	623.24	1.04
624.18	1.03	631.15	1.03	636.21	1.03
640.18	1.02	647.2	1.02	653.22	1.02
663.15	1.01	671.19	1.01	677.19	1.01
685.15	1.00	694.18	1.00	700.19	1.00
718.16	0.99	728.23	0.98	735.15	0.98
781.17	0.96	794.23	0.95	800.18	0.95
857.23	0.93	870.24	0.92	881.23	0.92

Our study includes the random nucleation process, ascertained by experimental z(α) master plots. During the starting phase of such nucleation, the first nuclei appear randomly**,** and during the formation of such nuclei, the steadiness in the nucleation is only possible when the formed nuclei size (r) is equal to the standard critical size of nucleation (r*), as shown by the Equation below -

$$r^* = \frac{2\beta_a \gamma v}{3\beta_v k_B T ln(S)} \qquad (1)$$

Where, β_a is 4π, β_v It is $4\pi/3$, γ is abbreviated as surface free energy per unit area, v is the specific volume of the nanomaterial, T is the specific Temperature, and S is supersaturation. At a specific temperature, the first nucleus appears when the radius of the nuclei formed is equivalent to the standard critical size of nucleation, as described in Eq.(1), and the value of supersaturation (S) reaches 2.718. Our study includes the formation of first nuclei by the R3 mechanism, ascertained by $z(\alpha)$ master plots, as a starting point of nucleation (when actual nucleation starts). Thereby, this study includes the value of supersaturation (S) to be 2.718. Consequently, by putting the value of Boltzmann constant, interfacial energy, specific volume, specific Temperature, supersaturation value, and other constants like β_a and β_v, the size range of ultra-small gadolinium oxide nanoclusters at various temperature increments (ranging from 503.17K to 857.23 K) during the event of nucleation has been calculated by using Eq. (1) and is summarized in Table A5.

The criterion for the formation of a stable crystal nucleus is met only when the size of the formed nucleus (r) is equal to the standard critical size of nucleation (r*), according to the Eq. (1)

Section A2:

A confidence interval (CI) is an estimate's uncertainty level, a range of numbers. For investigating the real difference or experimental errors in activation energy between two conversion points, we need to compute the confidence interval between two conversion points. The steps are listed below:

1. We collected the thermogravimetric data at 10 °C, 15 °C, and 20 °C.
2. Now we computed the activation energy using non-isothermal models at each conversion point.
3. Then we calculated the standard deviation for computing the standard error for activation energy at each conversion point.
4. Now we computed the standard errors for the difference in activation energy using the formula listed below:

   SE = $(SE1^2 + SE2^2)^{1/2}$

Where SE1 and SE2 stand for standard errors of the activation energy at each conversion point, which represent the amount of uncertainty or variation in computed activation energy.

5. Finally, we have calculated the confidence interval for the difference in activation energy using the formula listed below:

   95% CI = (diffe ± t-value * SE)

   Where diffe is the difference in activation energy.

   t-value is a critical value for t distribution for CI, which fixed in our case is 2.77, and for computing t value, the degree of freedom (dfr) is calculated using the formula listed below:

   dfr = n1 + n2 – 2 Where n1 and n2 are sample size.

6. Further, if the calculated value of the confidence interval does not contain zero, then the change in activation energy is statistically significant.
7. Hence, from Table A6, it is clear that the calculated value of the confidence interval is not zero; then, we conclude that the change in activation energy between two conversion points is not in the range of experimental error, which further shows that the change is statistically significant

Table A6. Calculation of confidence interval at each conversion points.

Conversion (α)	E_α (3 TGA runs) *			E_α (Initial)*	Standard Deviation (SD)*	Standard Error (SE)*	95 %CI (Confidence interval)	CI (Zero/Non-Zero)	Statically Significant
	Exp 1	Exp2	Exp3						
0.05	67.41	67.55	67.44	67.41	0.073	0.042		Non-Zero	YES
0.1	134.6	136.58	136.47	134.6	1.11	0.64	(65.04, 68.97)	Non-Zero	YES
0.15	127.08	123.21	124.83	127.08	1.94	1.12	(11.10, 3.93)	Non-Zero	YES
0.2	150.10	146.55	146.55	150.10	2.04	1.18	(18.49, 27.54)	Non-Zero	YES
0.25	158.29	157.12	157.18	158.29	0.65	0.38	(4.73, 11.64)	Non-Zero	YES
0.30	150.63	147.27	148.06	150.63	1.75	1.01	(10.66, 4.65)	Non-Zero	YES
0.35	168.6	168.5	168.45	168.6	0.07	0.04	(15.15, 20.78)	Non-Zero	YES
0.40	169.21	169.56	169.43	169.21	0.17	0.10	(5.65, 13.92)	Non-Zero	YES
0.45	174.13	173.25	176.67	174.13	1.77	1.02	(2.05, 7.78)	Non-Zero	YES
0.5	177.9	176.67	177.32	177.9	0.61	0.35	(0.75, 6.78)	Non-Zero	YES
0.55	181.82	181.15	184.89	181.82	1.99	1.15	(0.57, 7.26)	Non-Zero	YES
0.60	187.97	187.68	190.24	187.97	1.40	0.80	(2.24, 10.05)	Non-Zero	YES
0.65	180.04	182.38	179.47	180.04	1.54	0.89	(11.27, 4.58)	Non-Zero	YES
0.70	174.79	174.90	175.11	174.79	0.16	0.09	(7.73, 2.76)	Non-Zero	YES
0.75	173.64	174.60	174.1	173.64	0.48	0.27	(5.43, 10.5)	Non-Zero	YES
0.80	172.12	173.20	172.50	172.12	0.54	0.31	(2.68, 0.35)	Non-Zero	YES
0.85	167.07	167.62	168.08	167.07	0.50	0.29	(6.24, 3.85)	Non-Zero	YES
0.90	171.83	176.40	175.43	171.83	2.40	1.39	(0.81, 8.70)	Non-Zero	YES
0.95	167.89	168.40	168.10	167.89	0.25	0.14	(7.82, 0.05)	Non-Zero	YES

*All the values of activation energy, standard deviations and standard errors are in **kJ/mol.**

Appendix B

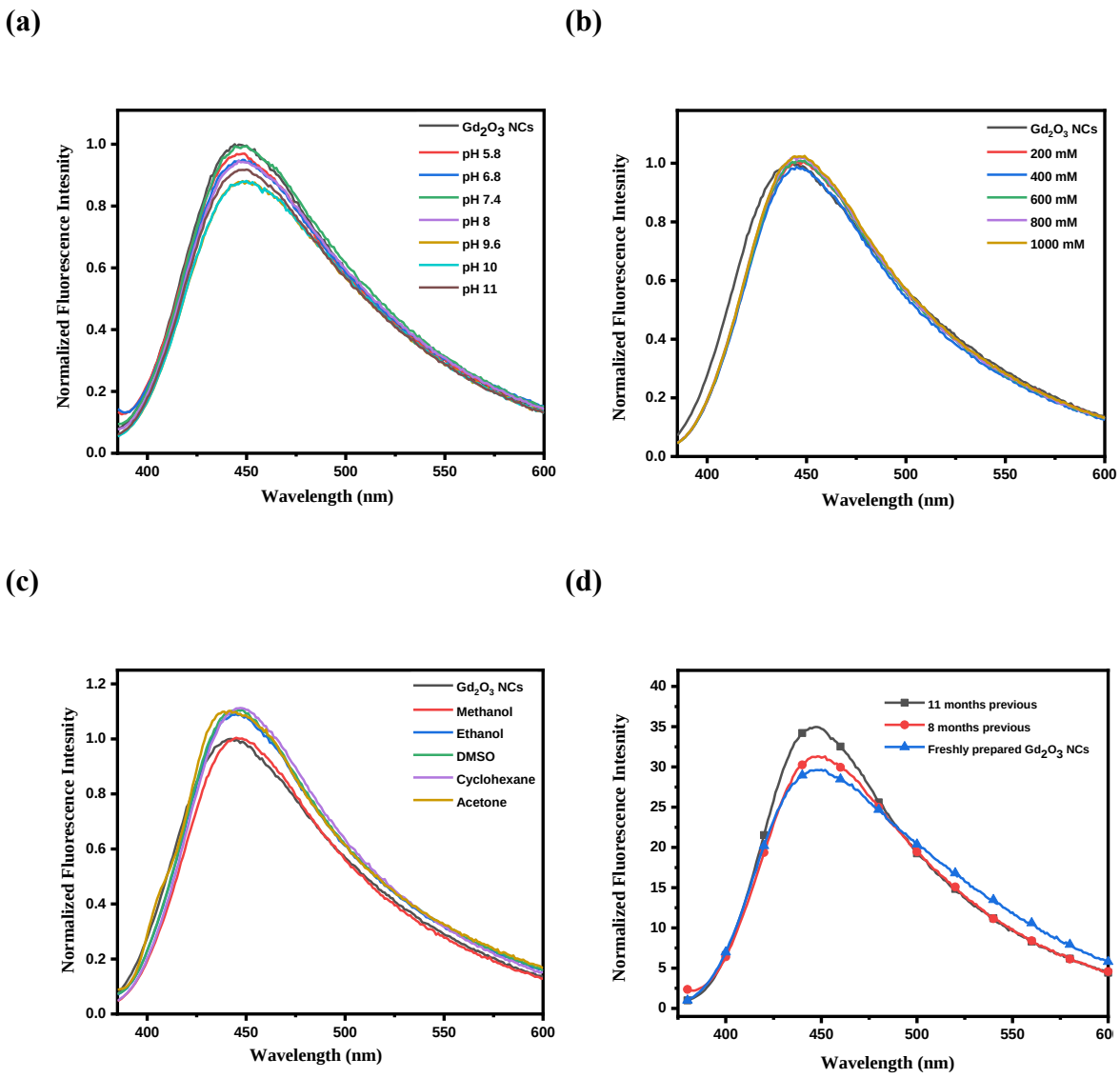

Figure B1: (a) pH. dependent normalized fluorescence emission spectra at different pH. (5.8-11) at λ_{Ex} 365 nm, (b) Normalized fluorescence emission spectra for Gd_2O_3 NCs after the addition of various concentrations of freshly prepared NaCl solution at λ_{Ex} 365, (c) Normalized fluorescence emission spectra of freshly prepared Gd_2O_3 NCs with different solvent at λ_{Ex} 365, (d) Normalized fluorescence emission spectra for freshly prepared Gd_2O_3 NCs, previous 8 months and nearly 11 months old at λ_{Ex} 365.

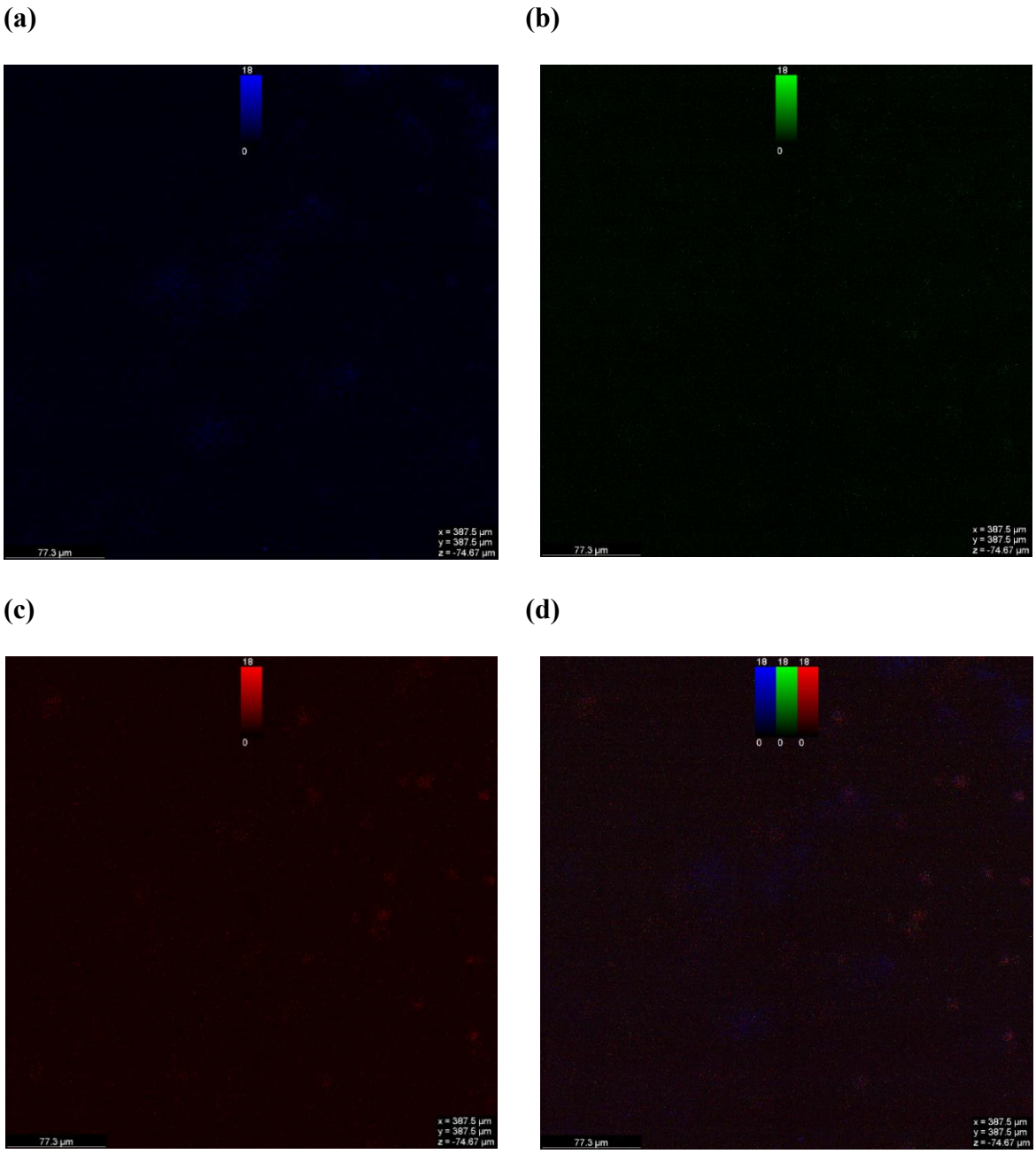

Figure B2: Multifluorescent confocal image of U 87-MG cells treated with Chitosan polymer.

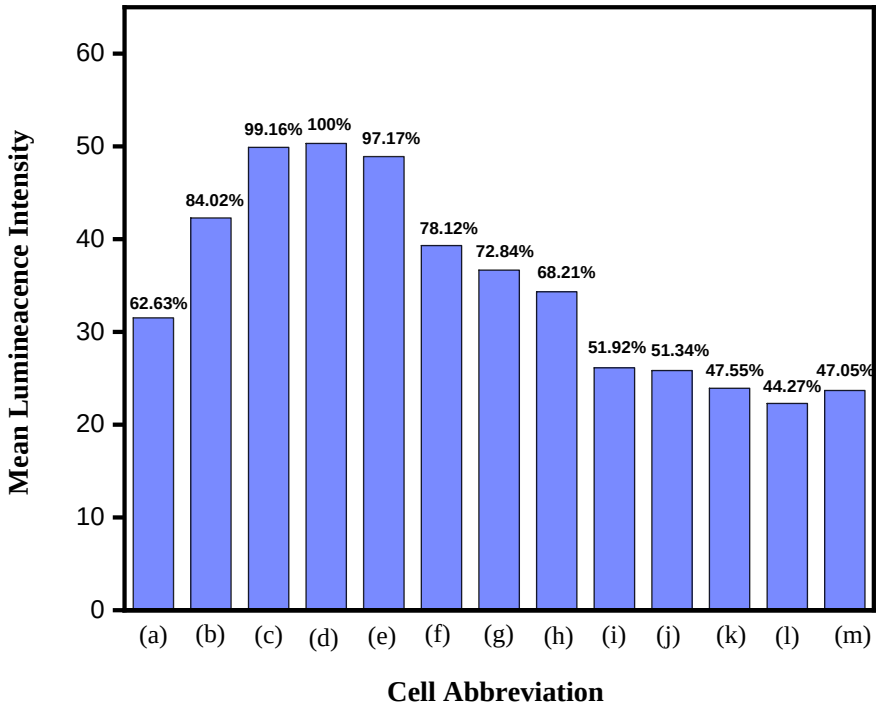

Figure B3: Mean Luminescence Intensity with Cell depth penetration in U87-MG cell line at λ_{Ex} 366 nm. Where (a) = 0 µm, (b) = 2µm, (c) = 4µm, (d) = 6µm, (e) = 8µm, (f) = 10µm, (g) = 12µm, (h) = 14 µm, (i) = 16 µm, (j) = 18 µm, (k) = 20 µm, (l) = 22 µm, (m) = 24 µm.

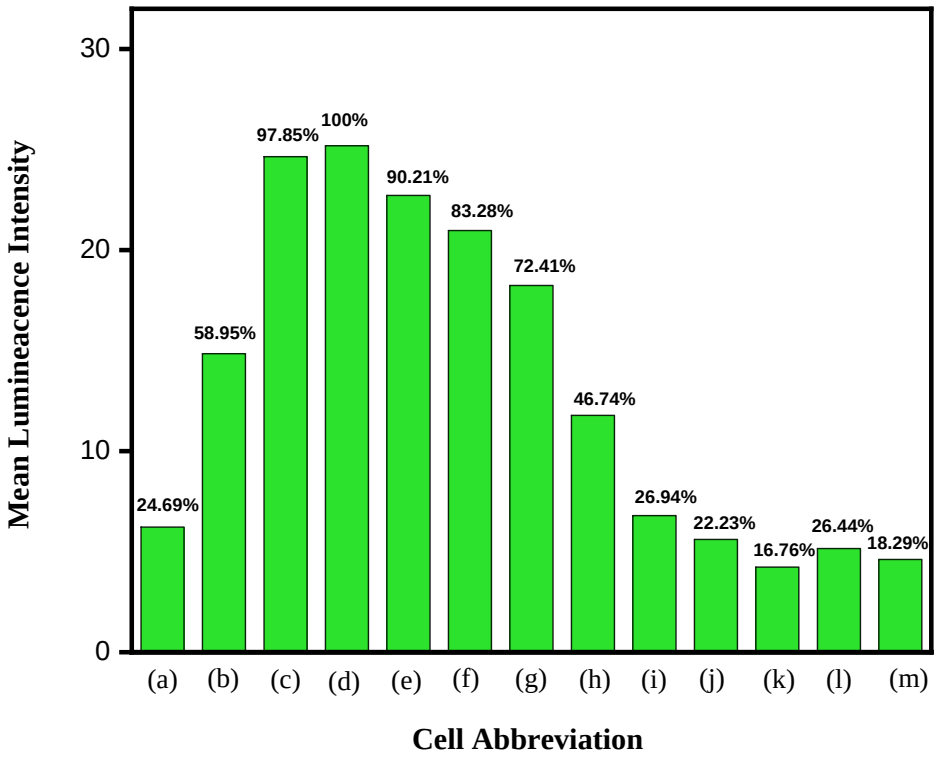

Figure B4: Mean Luminescence Intensity with Cell depth penetration in U87-MG cell line at λ_{Ex} 472 nm. Where (a) = 0 µm, (b) = 2µm, (c) = 4µm, (d) = 6µm, (e) = 8µm, (f) = 10µm, (g) = 12µm, (h) = 14 µm, (i) = 16 µm, (j) = 18 µm, (k) = 20 µm, (l) = 22 µm, (m) = 24 µm.

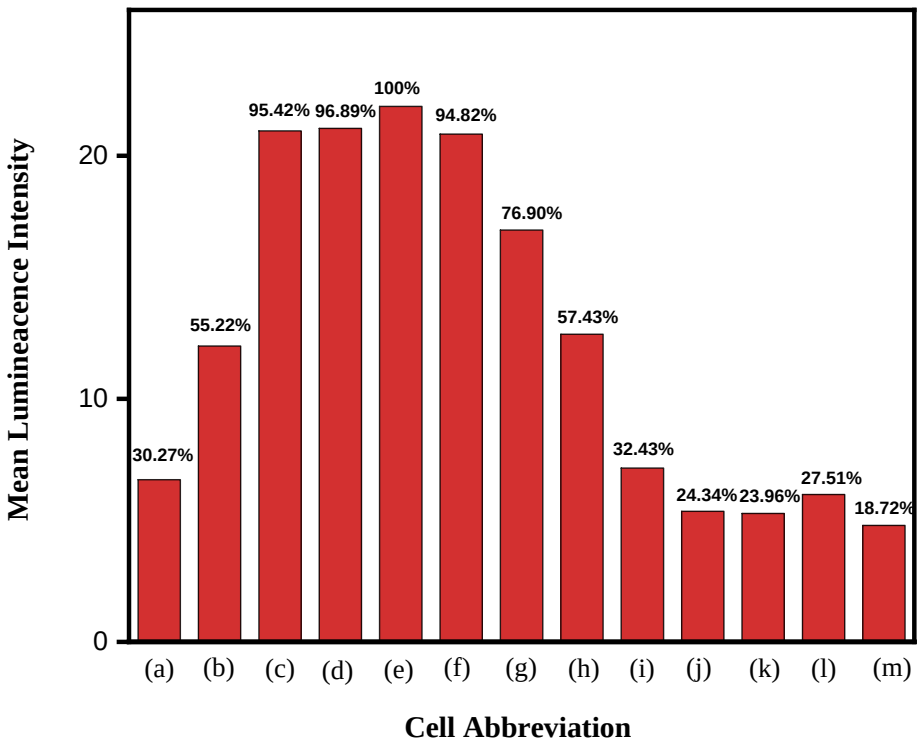

Figure B5: Mean Luminescence Intensity with Cell depth penetration in U87-MG cell line at λ_{Ex} 472 nm. Where (a) = 0 µm, (b) = 2µm, (c) = 4µm, (d) = 6µm, (e) = 8µm, (f) = 10µm, (g) = 12µm, (h) = 14 µm, (i) = 16 µm, (j) = 18 µm, (k) = 20 µm, (l) = 22 µm, (m) = 24 µm.

Appendix C

(a)

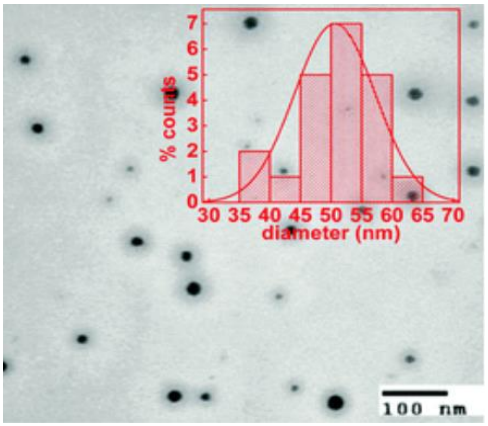

(b)

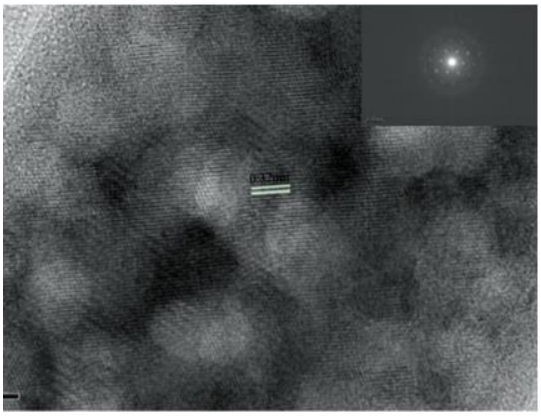

(c)

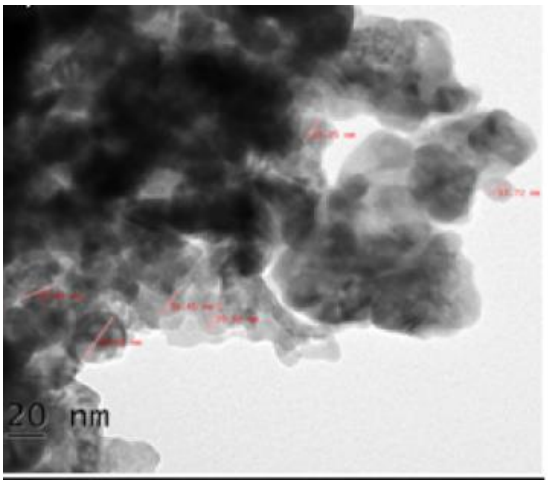

(d)

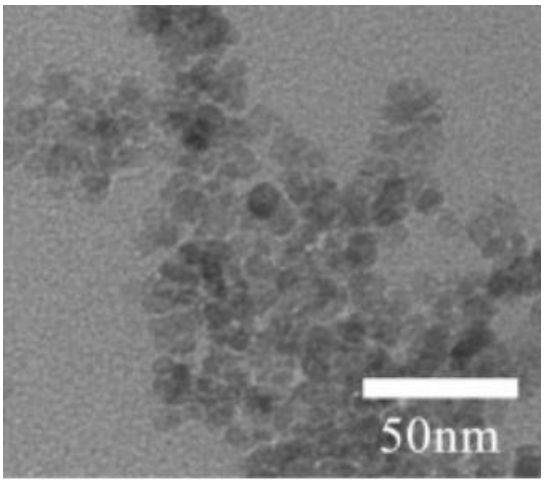

Figure C1: Representative image for TEM for various Gd_2O_3 nanomaterials from table 2.1 (a) Ref.217, (b) Ref. 219, (c) Ref.220, (d) Ref. 221.

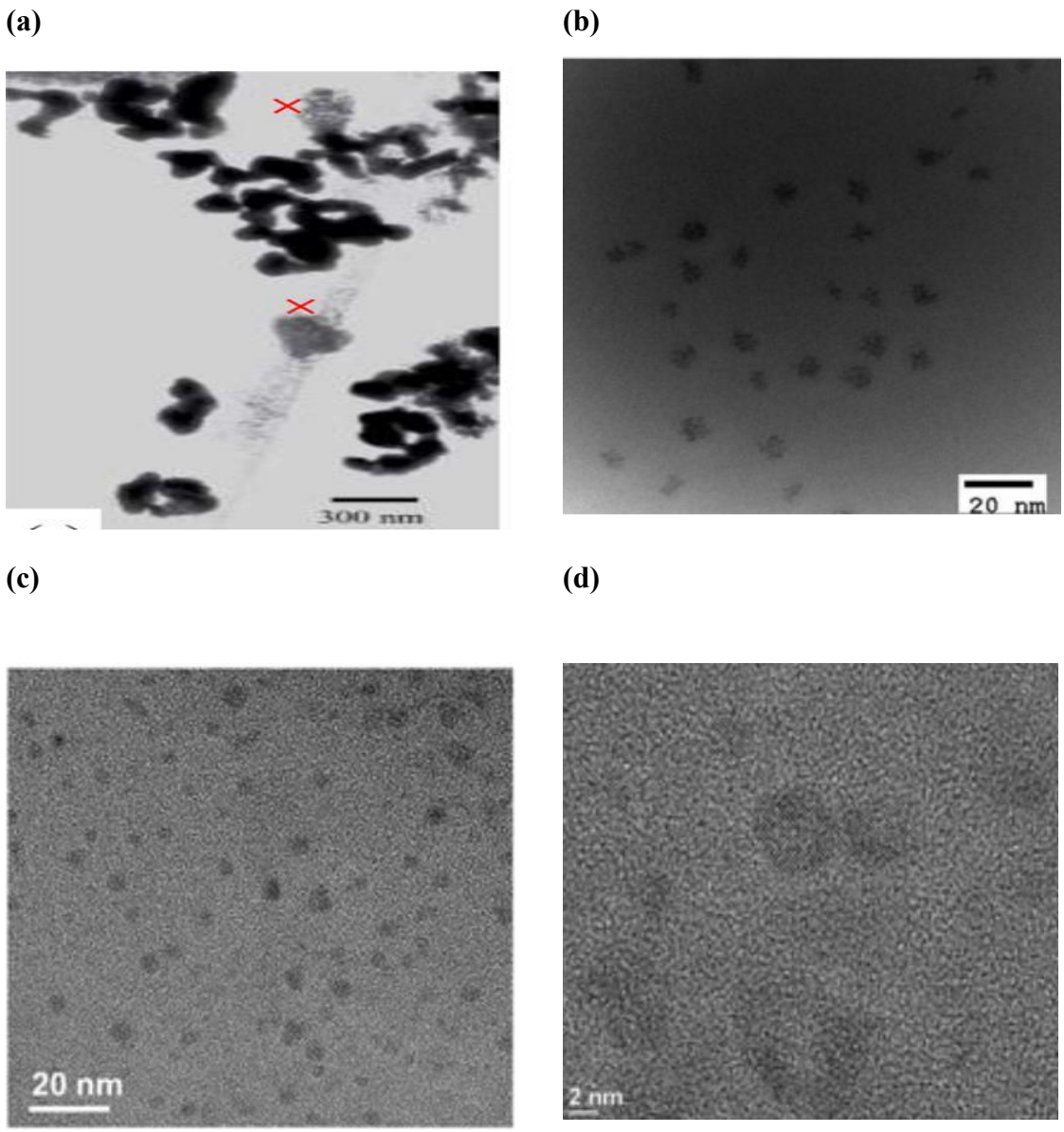

Figure C2: Representative image for TEM for various Gd_2O_3 nanomaterial from table 2.1 (a) Ref.223, (b) Ref. 224, (c) Ref.225, (d) Ref. 229.

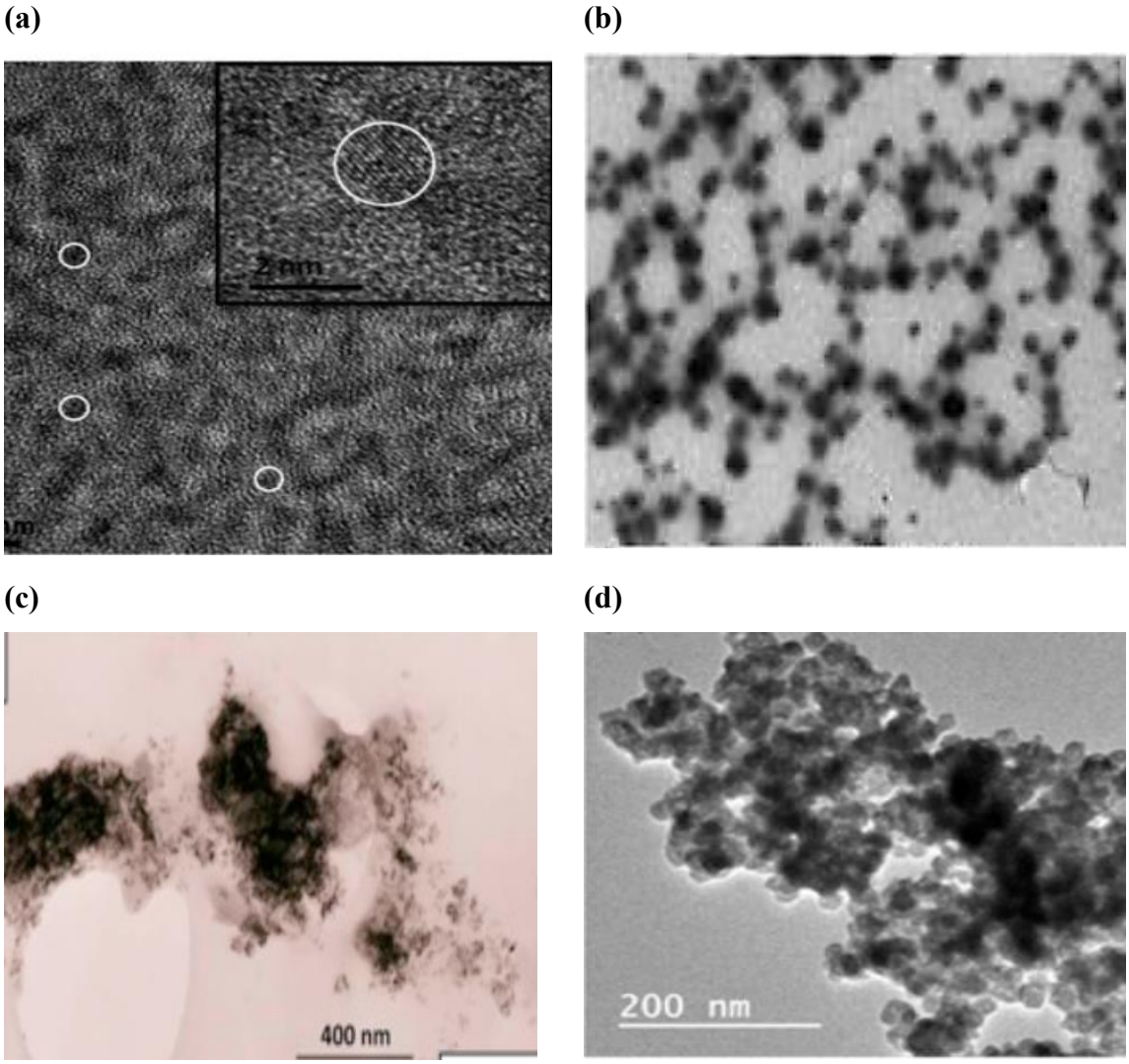

Figure C3: Representative image for TEM for various Gd_2O_3 nanomaterial from table 2.1 (a) Ref.231, (b) Ref. 232, (c) Ref.233, (d) Ref. 234.

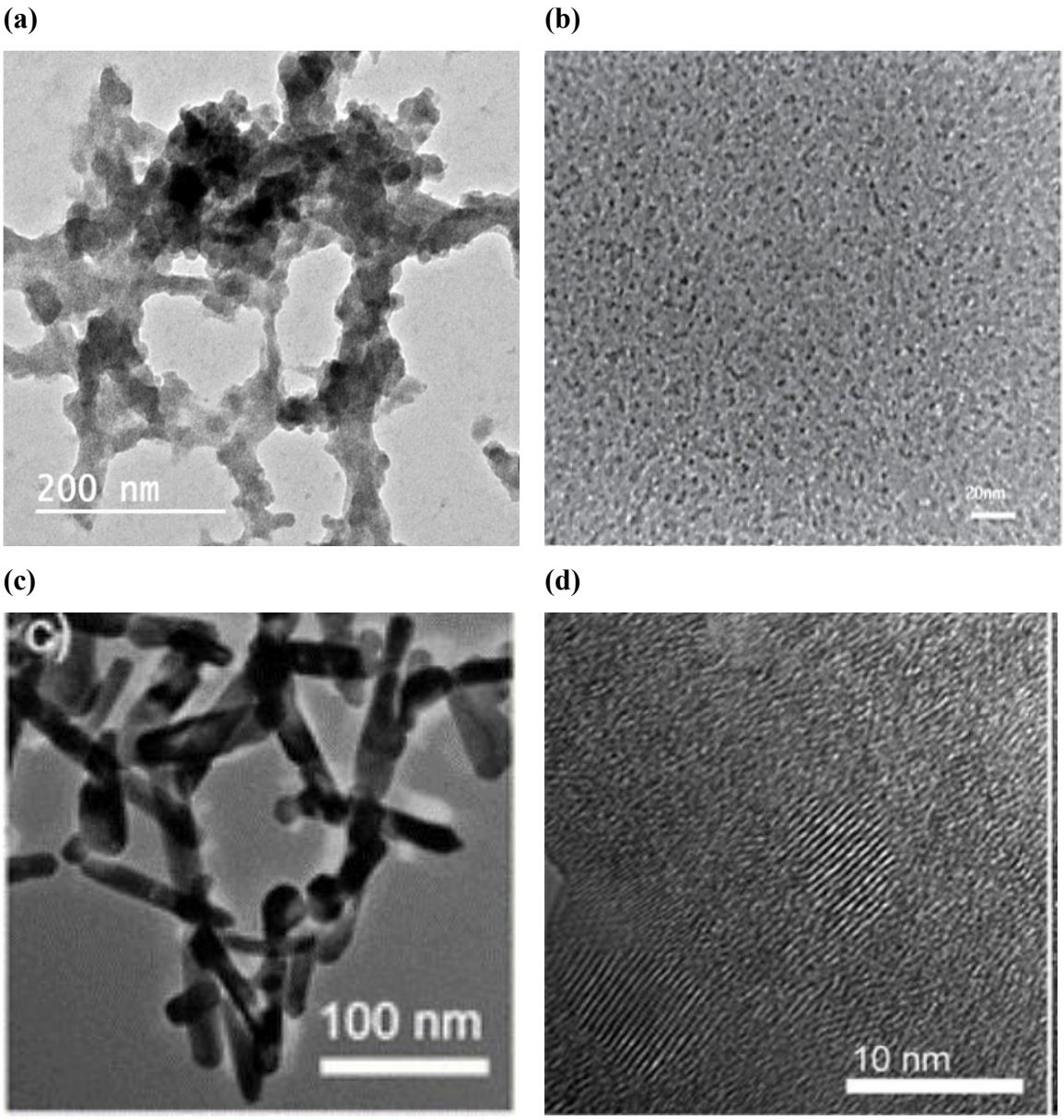

Figure C4: Representative image for TEM for various Gd_2O_3 nanomaterial from table 2.1 (a) Ref.235, (b) Ref. 237, (c) Ref.239, (d) Ref. 206.

1. **Vivek Kumar Verma**, Prachi Srivastava, Shivesh Sabbarwal, Mamata Singh, Dr. Biplob Koch, Dr. Manoj Kumar "White Light Emitting Gd_2O_3 Nanoclusters for In-vitro Bioimaging". ChemistrySelect I.F 2.3.
2. **Vivek Kumar Verma**, Shivesh Sabbarwal, Prachi Srivastava, Dr. Manoj Kumar "In-Depth Insight of Thermodynamic and Kinetic Barrier for Computation of Nucleation Rate and Interfacial Energy of Ultra-Small Gd_2O_3 Nanoclusters Utilizing Non-Isothermal Thermogravimetric Models". Physica Scripta I.F 3.1.
3. **Vivek Kumar Verma**, Prachi Srivastava, Abhisesh Kumar Mehata, Mamata Singh, Dr. M. S. Muthu, Dr. Biplob Koch, Dr. Manoj Ranjan, Dr. Manoj Kumar "One-pot synthesis of ultra-fine but ultra-effective Chitosan targeted gadolinium oxide nanocluster for multimodal imaging" Colloids and Surfaces B: Biointerfaces. I.F 6.4 (submitted).
4. Prachi Srivastava, **Vivek Kumar Verma**, Shivesh Sabbarwal, Mamata Singh, Kedar Sahoo, Dr. Biplob Koch, Dr. Manoj Kumar. "White Light Emitting, Biocompatible, Water Soluble Metallic Magnesium Nanoclusters for Bioimaging Applications." Nanotechnology I.F 3.99.
5. Prachi Srivastava, Shivesh Sabbarwal, **Vivek Kumar Verma**, Dr. Manoj Kumar "A novel approach for determination of Nucleation Rates and Interfacial Energy of Metallic Magnesium Nanoclusters at High Temperature using Non-isothermal TGA Models." Chemical Engineering Science (2022): 118223. I.F 4.89
6. Samarpita das; Pooja Goswami; **Vivek Kumar Verma**; Harish K. Indurthi; Manoj Kumar; Biplob Koch Deepak Kumar "Rapid Access to 7-substituted cycloalkylamino and alkylamino analogues of 4-methylcoumarin reveals surprising emitters" Dyes and Pigments IF **5.12**

7. Shivesh Sabbarwal, Prachi Srivastava, **Vivek Kumar Verma**, Dr. Manoj Kumar "New Approach to Calculate the Kinetic and Thermodynamic Barriers for Computation of Nucleation Rates and Interfacial Energy of $CaCO_3$ Prenucleation Nanoclusters at High Temperature using TGA models and their In-Situ Crystallization" Crystal Research and Engineering I.F 1.6
8. Shilpi Verma, Prachi Srivastava, **Vivek Kumar Verma**, Dr. Sangeeta Singh "In silico potential drug target identification against 4aminobutyrate aminotransferase for Huntington disease "Journal of Drug and Discovery 2017; 4(3): IISN: 23499036.
9. Shivesh Sabbarwal, **Vivek Kumar Verma**, Shreyashi Majumdar, Prachi Srivastava, Manoj Kumar "A Facile Synthesis of Nanodiamond Sn nanocrystals at room temperature with their beta phase for in-vitro photothermal cancer research. in-vivo toxicology and integrated Fourier transform modeling" ACS Material Letter I.F 8.4 (Under review)
10. Prachi Srivastava, **Vivek Kumar Verma**, Dr. Biplob Koch, Dr. Manoj Kumar" Design and development of Ag3Mg bimetallic nanoparticles as antimicrobial synergistic combination therapies against clinically relevant pathogens and anticancerous activity via plasmonic heating" Nanoscale. IF 10.5 (Submitted)
11. Prachi Srivastava, **Vivek Kumar Verma**, Deepa Dehri, Dr. A K Agrwal, Dr. Manoj Kumar," Essential oil mediated synthesis of angiogenetic Magnogel against clinically relevant pathogens microbes" Colloids and Surfaces B: Biointerfaces. IF 5.8 (Submitted)
12. Prachi Srivastava, **Vivek Kumar Verma**, Abhisesh Kumar Mehata, Mamata Singh, Dr. M. S. Muthu, Dr. Biplob Koch, Dr. Manoj Kumar, et al." Lysozyme templated

synthesis of metallic magnesium nanoparticles and their potential application in-vitro brain cell imaging and In vivo imaging system (IVIS).” Colloids and Surfaces B: Biointerfaces. IF 5.9 (Submitted).

भारतीय प्रौद्योगिकी संस्थान
काशी हिन्दु विश्वविद्यालय
IIT
INDIAN INSTITUTE OF TECHNOLOGY
BANARAS HINDU UNIVERSITY

Department of Pharmaceutical Engineering & Technology

Regd. No. 2123/GO/Re/S/21/CPCSEA Date: 03 May, 2022

IAEC Approval Number: **IIT(BHU)/IAEC/2022/077**

CERTIFICATE

This is to certify that the project proposal entitled ***"*Design and development of nanoparticle and fluorescence Nano-systems for possible application in health care*"*** submitted by **Mr. Vivek Kumar Verma** under supervision of **Dr. Manoj Kumar** has been approved/recommended by the IAEC of *Indian Institute of Technology, Banaras Hindu University, Varanasi* in its meeting dated **03/05/2022** and has been sanctioned **36 Male/Female Wistar Rats (200-250 gm), 18 Male/Female Swiss Albino Mice (20-25 gm)** under this proposal for a duration of **Twelve (12) months.**

Prof. Sushant Kumar Shrivastava	Dr. Vinod Tiwari	Dr. Shesh Narayan Mishra
Name & Signature	**Name & Signature**	**Name & Signature**
Chairman	**Member Secretary**	**Main Nominee of CPCSEA**

Note: The CPCSEA Guideline should be followed strictly while handling the animals